https://doi.org/10.5194/egusphere-2026-3441
Preprint. Discussion started: 25 June 2026
© Author(s) 2026. CC BY 4.0 License.

Advancing meteorite impact chronology with in situ mica Rb-Sr dating

Bruno V. Ribeiro[1,2*], Jayden Squire[3], Christopher L. Kirkland[1], Juraj Farkas[3], Cecilia Loyola[3], Victoria Cousins[1], Victor Gostin[3], Charles Verdel[4]

[1]School of Earth & Planetary Science (Timescales of Mineral Systems Group), Curtin University, Perth, Western Australia 6102, Australia

[2]John de Laeter Centre, Curtin University, Perth, Western Australia 6102, Australia

[3]School of Physics, Chemistry and Earth Sciences, Adelaide University, Adelaide, SA 5005, Australia

[4]Northern Territory Geological Survey, NT Government, Alice Springs, Northern Territory, 0870, Australia

*Corresponding author

Dr Bruno Vieira Ribeiro

bruno.vieiraribeiro@curtin.edu.au

https://doi.org/10.5194/egusphere-2026-3441
Preprint. Discussion started: 25 June 2026
© Author(s) 2026. CC BY 4.0 License.

ABSTRACT

Meteorite impacts are highly energetic processes that drives deformation on Earth under extreme pressure and temperature conditions, far exceeding those of typical crustal processes. Consequently, it may promote environmental perturbations, blossoming/extinction of life and even produce suitable conditions for the formation of mineral resources. Thus, constraining the timing of impacts is pivotal to shedding light on its role in Earth's biogeodynamics, yet less than ~20% of the impacts worldwide are precisely dated. Here, we present novel in situ mica Rb–Sr isotopes from the Australian Acraman and Gosses Bluff impact sites collected via LA-ICP-MS/MS, including single- and multi-collector instruments to expand the chronological toolbox for dating meteorite impacts. Whilst monazite (980 ± 28 Ma) and apatite (1448 ± 79 Ma) yield older ages compared to the expected Acraman impact age of 588 ± 35 Ma, in situ Rb–Sr from muscovite-bearing domains from the Acraman ejecta layer (580 ± 8 Ma; multi-collector age) and associated fine-grained zircon (598 ± 16 Ma) are consistent with the expected impact age. Similarly, apatite (132 ± 14 Ma) and mica-bearing domains (137 ± 9 Ma; multi-collector age) are comparable to the proposed impact age of 133 ± 3 Ma, whilst zircon yields mostly discordant data. The Rb–Sr results comparison between single- and multi-collector ICP-MS/MS has shown that the latter yielded significantly more precise Sr measurements, likely due to measurement of St isotopes with high resistor Faraday cups (10^{13} Ω) resulting in improved signal-to-noise ratio, consequently yielding more precise isotopic ratios and isochron ages. Our findings show that in situ Rb–Sr dating of micas formed during impact metamorphism offers the means for determining the timing of meteorite impact events. This approach effectively addresses the textural complexities commonly present in impact-related rocks, which are often overlooked by bulk isotope-dilution techniques, and delivers accuracy sufficient to establish the age of impacts. The effectiveness of in situ Rb–Sr dating of impact-related micas may be attributed to their higher resistance to hydrothermal alteration compared to Ar isotopes, which often yield complex degassing spectra and younger apparent ages such as for the Acraman impact. This study shows that in situ Rb–Sr isotopes of newly grown micas in impact-related rocks refines the chronology of impacts, with potential to increase the number of dated impacts globally with a low-cost, speedy technique with minimum sample preparation. Such task is crucial for understanding the role of meteorite impacts, including their potential influence on environmental crises, mass extinctions, and the emergence of life.

https://doi.org/10.5194/egusphere-2026-3441
Preprint. Discussion started: 25 June 2026
© Author(s) 2026. CC BY 4.0 License.

1. Introduction

The Earth is one of the several planetary bodies within the solar system that is subject to interaction with extraterrestrial bodies, producing meteorite impacts on the Earth's surface if these bodies survive the extreme atmospheric conditions on Earth. Some meteorite impacts are known for their destructive potential, such as the Chicxulub impact in the Yucatán Peninsula (Mexico), potentially resulting in global consequences that could reshape ecosystems and the environment with mass extinctions (Artemieva and Morgan, 2017; Hildebrand et al., 1991; Schulte et al., 2010). Conversely, while locally and immediately catastrophic, these changes can create favorable environmental conditions for the blossoming of primordial life (Cockell et al., 2002; Collins et al., 2012; Osinski et al., 2020). 2020) and hosting economically significant mineral systems (Hayward et al., 2005; Reimold et al., 2005; Tuchscherer and Spray, 2002). Importantly, knowing the timing of the impact formation is essential to unravel its role in earth systems evolution and the Earth's biological history (Jourdan et al., 2012, 2009; Osinski et al., 2022)

Establishing the timing of impact structures remains a significant challenge, with fewer than 20% of known examples yielding radiometric ages precise to within 2% uncertainty (French and Koeberl, 2010; Quintero et al., 2021). The last revision of the Australian impacts has shown that only five out of 31 confirmed impact craters/structures have well-constrained radiometric age (Quintero et al., 2021). Obtaining such constraints is complicated by the enormous energy released during impacts, subjecting rocks to extreme pressure–temperature deformation conditions far exceeding those of typical crustal processes (Collins et al., 2012; Timms et al., 2017). Rock deformation at these conditions generates profound mineralogical and chemical–isotopic complexities in key gold-standard geochronometers such as zircon and monazite, often resulting in incomplete isotopic resetting and intricate age spectra of difficult interpretation (e.g., Guerrero et al., 2025; Herrmann et al., 2024; McGregor et al., 2019). Thus, there is a pressing need to broaden the geochronological toolbox by developing novel approaches to easily

https://doi.org/10.5194/egusphere-2026-3441
Preprint. Discussion started: 25 June 2026
© Author(s) 2026. CC BY 4.0 License.

accessible rock-forming minerals like micas and feldspars, which may provide robust temporal constraints on meteorite impact events.

Here, we test a novel approach to date fine-grained micas from shock-related rocks from the Australian Acraman and Gosses Bluff (Tnorala) impacts via in situ Rb–Sr geochronology carried out using single- and multi-collectors instruments for the first time. This comparison allowed us to test the accuracy and precision of each analytical approach to expand the geochronological toolbox currently used for dating terrestrial impacts.

2. Background

The Acraman impact structure displays a circular structure of ~30 km diameter within the Proterozoic volcanics in the Gawler Ranges (Williams, 1992, 1986). The volcanics rocks that underwent impact deformation exhibit shatter cones and shock lamellae (planar deformation feature) in quartz, suggesting shock pressures higher than 15 GPa (Williams, 1992, 1986). The Acraman impact has been suggested to be a trigger for environmental crisis in the Late Vendian spanning 600–543 Ma, a known period of increased diversification of fossil assemblages prior to the Cambrian explosion (McCall, 2006), based on its size and estimated impact energy (Williams and Wallace, 2003). Yet, chronological data from the impact rocks has either yielded the protoliths' ages, or younger orogenic resetting events (Compston et al., 1987; Schmieder et al., 2015), whilst step-heating K-Ar and $^{40}Ar/^{39}Ar$ analyses of quartz-feldspar bearing melt rocks from the center of the Acraman structure yielded complex degassing patterns and age estimates younger than ca. 450 Ma (Baldwin et al., 1991; Jourdan, 2012; Schmieder et al., 2015), interpreted as the timing of rock alteration post-impact. Currently, the Acraman structure is stratigraphically constrained between 625–570 Ma (Hill et al., 2007). The suggested age of the Acraman event comes from the distinct ejecta layer that is prominent in parts of the Adelaide Superbasin and the Officer Basin (Gostin et al., 1986), with the host unit yielding a whole-rock Rb–Sr age of 588 ± 35 (Webb et al., 1983). However, the robustness of this age remains to be assessed since it has only been mentioned in a conference abstract.

https://doi.org/10.5194/egusphere-2026-3441
Preprint. Discussion started: 25 June 2026
© Author(s) 2026. CC BY 4.0 License.

Gosses Bluff is a world-known impact structure located within the northern part of the Paleozoic Amadeus Basin in Central Australia (Northern Territory). This structure represents an eroded complex crater of an estimated ~24 km diameter that underwent extensive erosion exposing a circular rim of ~5 km in diameter (Milton et al., 1972; Milton and Sutter, 1987). The circular structure is hosted in flat-lying sedimentary sequences (including sandstones, shales and limestones), displaying abundant evidence of impact metamorphism including shatter cones and quartz sandstones with obliterated sedimentary fabric containing quartz displaying planar deformation features (Crook and Cook, 1966; Dietz, 1967). Impact melt breccias composed of mosaic fine-grained quartz and micas with locally rounded quartz grains (i.e., partly recrystallized sandstone) and devitrified glassy rocks (including melt-pellets) displaying fine-grained quartz, micas and feldspars are common in the Gosses Bluff structure (Milton and Sutter, 1987). Pioneer chronological constraints produced via total fusion K-Ar of sanidine-rich suevite (133 ± 3 Ma) and zircon fission track (130 ± 6 Ma) from a sandstone beneath the melt breccia suggested a Lower Cretaceous age for the formation of the Glosses Bluff impact structure (Milton et al., 1972). Subsequently, (Milton and Sutter, 1987) proposed an older impact formation date of 142.5 ± 0.8 Ma based on total fusion $^{40}Ar/^{39}Ar$ dating of pumiceous suevite clasts from the melt breccia composed of fine-grained sanidine, potentially linking the formation of the Gosses Bluff impact with the Jurassic–Cretaceous stratigraphic boundary. Yet, the older age should be treated with caution given the discordant and complex ^{39}Ar spectrum. Similar complex $^{40}Ar/^{39}Ar$ spectrum were produced from the analyses of similar rocks (Jourdan, 2012), which were interpreted to reflect a ^{40}Ar Fickian diffusion profile converging towards c. 145 Ma interpreted as a minimum age for the Gosses Bluff impact. Despite the multiple attempts, a temporal link between this impact with the Jurassic-Cretaceous stratigraphic boundary remain unresolved.

Notably, the Acraman and the Gosses Bluff impact structures were tentatively dated via total fusion K-Ar and $^{40}Ar/^{39}Ar$ analyses of whole-rock specimens, dismissing the mineralogical and microstructural diversity of such rocks resulting in complex results. Here, we attempt to address

https://doi.org/10.5194/egusphere-2026-3441
Preprint. Discussion started: 25 June 2026
© Author(s) 2026. CC BY 4.0 License.

this problem by applying novel in situ Rb–Sr geochronology by targeting mica-bearing domains in ejecta layer from the Acraman and melt-pellets from the Gosses Bluff impact structures to tentatively determine the timing of impact deformation. This chronological approach accounts for the variable textural components on such complex rocks, opening a new field in the chronology of impact processes.

3. Methods

3.1. Automate mineralogy mapping

The samples were scanned with a TESCAN Integrated Mineral Analyzer (TIMA) at Curtin University's John de Laeter Centre to characterize the mineral assemblage, focusing on micas in the Acraman and Gosses Bluff samples. The TIMA is an automated scanning electron microscopy system that integrates quantitative EDS analysis and a statistical approach that can obtain up to 500 spectra per second (Hrstka et al., 2018), which is further combined with backscatter electron (BSE) images providing high-resolution mineralogy, chemistry and textural data. The analyzes were carried out with an accelerating voltage of 25 kV, beam intensity of 19.8, probe current of 7.15 nA, spot size of 124 nm, field size of 1000 µm and working distance of 15 mm. A pure Mn standard was used for EDS spectra standardization.

3.2. In situ Rb–Sr geochronology

Impact-related samples from the Acraman and Gosses Bluff were dated via in situ Rb–Sr geochronology through different analytical approaches to evaluate instrument sensitivity and further implications to isotopic ratio uncertainties, including single-quadrupole tandem-ICP-MS/MS and multi-collector tandem-ICP-MS/MS. The Rb–Sr isochrons and ages were calculated using the maximum likelihood model in IsoplotR (Vermeesch, 2018) with the ^{87}Rb decay constant from Villa et al. (2015). Dates and uncertainties are presented at 2-standard error (2SE).

3.2.1. Single-collector ICP-MS/MS (Adelaide Microscopy, Adelaide University)

The protocol employed at Adelaide Microscopy (University of Adelaide) includes RESOlution ArF excimer LA system (193 nm) coupled to an Agilent 8900 triple quadrupole in MS/MS mode

https://doi.org/10.5194/egusphere-2026-3441
Preprint. Discussion started: 25 June 2026
© Author(s) 2026. CC BY 4.0 License.

with N_2O (Hogmalm et al., 2017; Zack and Hogmalm, 2016). The analyses were carried out using a 67 µm circular beam diameter, 5 Hz repetition rate and a laser fluence of ~3.5 J.cm^{-2} measured above the cell prior to the analytical session. The international reference glass NIST SRM 610 with known $^{87}Rb/^{86}Sr$ and $^{87}Sr/^{86}Sr$ ratios (Woodhead and Hergt, 2001) was employed as primary reference material for normalization and instrumental drift correction, while MDC phlogopite (Redaa et al., 2021a) is used as the matrix matched secondary reference material for $^{87}Rb/^{86}Sr$ correction. Entire Creek biotite and Robins Folly muscovite (Milton et al., 1972; Milton and Sutter, 1987) were employed as secondary reference materials and treated as unknowns to account for secondary age checks.

Data reduction was carried out using LADR to determine drift-corrected $^{87}Rb/^{86}Sr$ and $^{87}Sr/^{86}Sr$ isotopic ratios (Redaa et al., 2021a) employing NIST SRM 610 (Woodhead and Hergt, 2001) as primary reference materials. Matrix correction was carried out offline using the MDC phlogopite (reference age of 519.4 ± 6.5; Redaa et al., 2021a). Secondary reference materials such as the Robins Folly muscovite and Entire Creek biotite yielded matrix-corrected isochron ages of 320 ± 10 (MSWD = 1.3, N = 25) and 311 ± 8 (MSWD = 0.1, N = 24), respectively, in agreement with reference ages.

3.2.2. Single-collector ICP-MS/MS (GeoHistory Facility; Curtin University)

The analytical setup in the GeoHistory Facility includes a RESOlution 193 nm ArF excimer laser with a Laurin Technic S155 sample cell coupled to an Agilent 8900 triple quadrupole mass spectrometer in MS/MS mode using the N_2O in the reaction cell (Hogmalm et al., 2017). The analyses were carried out using a 90 µm circular beam diameter, 7 Hz repetition rate and a laser fluence of ~2.8 J.cm^{-2} measured above the cell prior to the analytical session. A 'squid' mixing device (Laurin Technic) was used to smooth the aerosol pulses between the laser and mass spectrometer. Instrument tunning was performed using NIST SRM 610 glass in single quadrupole (no-gas mode) to optimize plasma conditions, minimize oxide interferences and maximize ^{85}Rb sensitivity. After shifting to MS/MS mode, the ICP-MS was tuned to maximizing sensitivity for SrO^+

https://doi.org/10.5194/egusphere-2026-3441
Preprint. Discussion started: 25 June 2026
© Author(s) 2026. CC BY 4.0 License.

reaction products. Ablation was performed in a He atmosphere (320 ml.min^{-1}), mixed with Ar (1 l.min^{-1}), and a low flow of N_2 (4 ml.min^{-1}) was added to the carrier gas before the ICP torch to enhance sensitivity (Hu et al., 2008).

Data reduction was performed in Iolite 4 (Paton et al., 2011a) using an in-house data reduction scheme adapted from Redaa et al. (2021). The $^{87}Sr/^{86}Sr$ and $^{87}Rb/^{86}Sr$ ratios were drift-corrected and calibrated against NIST SRM 610 with recommended isotopic ratios from Woodhead and Hergt (2001). and further matrix correction was carried using an isochronous calibration based on the Rb-Sr from LaPosta biotite (e.g., Giuliani et al., 2024). Unknowns were additionally bracketed with Mount Dromedary biotite (Rösel and Zack, 2022). Matrix-corrected Mount Dromedary returned an isochron date of 99 ± 3 Ma (n = 32, MSWD = 1.4) considering an initial $^{87}Sr/^{86}Sr$ of 0.70446 (c.f., Rösel and Zack, 2022).

3.2.3. Multi-collector ICP-MS/MS (GeoHistory Facility, Curtin University)

The approach utilized at the GeoHistory Facility (Curtin University) includes a Coherent LR laser ablation system (193 nm) equipped with a Lauren Technic S155 sample cell connected to a Thermo Fisher Neoma multi-collector inductively coupled plasma mass spectrometer (ICP-MS/MS) equipped with a reaction cell. The analyses were carried out across two analytical sessions using a 90 µm circular beam diameter, 7 Hz repetition rate and a laser fluence of ~2.8 J.cm^{-2} measured above the cell prior to the analytical session. A 'squid' mixing device (Laurin Technic) was used to smooth the aerosol pulses between the laser and mass spectrometer. Ablation was performed in a He atmosphere (320 ml.min^{-1}), mixed with Ar (1 l.min^{-1}), and a low flow of N_2 (3 ml.min^{-1}) was added to the carrier gas before the ICP torch to enhance sensitivity (Hu et al., 2008).

The mass spectrometer was run in MS/MS mode using SF_6 as reaction gas to facilitate simultaneous measurement of Rb and Sr isotopes (Bevan et al., 2021; Cruz-Uribe et al., 2023; Dauphas et al., 2022). All relevant masses from ^{85}Rb to $^{88}Sr^{19}F$ were measured for 140 integrations

https://doi.org/10.5194/egusphere-2026-3441
Preprint. Discussion started: 25 June 2026
© Author(s) 2026. CC BY 4.0 License.

for 0.5 s with a 30 s baseline acquisition, followed by a 30 s sample ablation and 10 s washout. The $^{86}Sr^{19}F$ (H3 cup) and $^{87}Sr^{19}F$ (H4 cup) analytes were measured in Faraday cups connected to 10^{13} Ω amplifiers to enhance signal to noise ratios, whereas all other analytes were measured in Faraday cups connected to 10^{11} Ω amplifiers. The peak center was positioned on the left shoulder of the time-resolved peak to reduce potential interferences from SF_3O and SF_3OH_2 on masses m/z 105 and 107.

Data reduction was performed in Iolite 4 (Paton et al., 2011) using an in-house data reduction scheme. The $^{87}Rb/^{86}Sr$ and $^{87}Sr/^{86}Sr$ were drift-corrected and calibrated against NIST SRM 612 (Woodhead and Hergt, 2001), and further matrix correction was carried using an isochronous calibration based on the Rb-Sr from Mount Dromedary biotite (e.g., Giuliani et al., 2024). The matrix offset as a correction factor to the $^{87}Rb/^{86}Sr$ ratios of samples and LaPosta biotite (secondary reference material). The matrix-corrected LaPosta returned an isochron date of 87 ± 4 Ma (n =13, MSWD = 0.2; session 1) and 92 ± 3 Ma (n = 26, MSWD = 0.4; session 2) in agreement with reference values (Rösel and Zack, 2022).

3.3. In situ U–Pb geochronology

We obtained apatite, zircon and monazite U–Pb data from the Acraman and Gosses Bluff impact to compare with new mica Rb–Sr ages.

The setup includes a Coherent LR laser ablation system (193 nm) equipped with a Lauren Technic S155 sample cell connected to an Agilent 8900 for the measurement of U–Pb isotopes. A 'squid' mixing device (Laurin Technic) was used to smooth the aerosol pulses between the laser and mass-spectrometer. The sample cell was flushed with ultrahigh purity He (320 $ml.min^{-1}$) and N_2 (1.0 $ml.min^{-1}$), both of which were passed through an inline Hg trap. The low flow rate of N_2 was added to the carrier gas before the ICP torch to enhance sensitivity (Hu et al., 2008).The samples and reference materials were ablated using a laser fluence of ~2.7 $J.cm^{-2}$, repetition rate of 10 Hz and a circular beam of 23 µm for apatite and zircon, and 15 µm for monazite. Each analysis consisted of 30 s of baseline acquisition, followed by 20 s sample ablation and 10 s fast

https://doi.org/10.5194/egusphere-2026-3441
Preprint. Discussion started: 25 June 2026
© Author(s) 2026. CC BY 4.0 License.

washout. Instrument tunning was performed using NIST SRM 610 glass to optimize plasma conditions, maximize instrument sensitivity and minimize oxide interferences.

Unknowns were bracketed by a suite of reference materials. Madagascar MAD-2 apatite (Thomson et al., 2012), zircon GJ-1 (Jackson et al., 2004) and Stern monazite (Horstwood et al., 2016) were employed as primary reference materials for U-Pb calibration. McClure Mountain (Schoene and Bowring, 2006) and FC-Duluth apatite (Apen et al., 2024; Schmitz et al., 2003; Thomson et al., 2012), zircon 91500 (Woodhead and Hergt, 2005) and Plesovice (Slama et al., 2008), and monazite 44069 (Aleinikoff et al., 2006) and Managotry (Montel et al., 1996) monazite were employed as secondary reference materials and treated as unknown. Data reduction was performed in Iolite4 (Paton et al., 2011) using an exponential with linear equation to account for U-Pb downhole fractionation. The U–Pb diagrams and dates were calculated using IsoplotR (Vermeesch, 2018), with ages and uncertainties being presented at the 2-standard error (2SE).

4. Results

4.1. Sample description

The ejecta layer sample from the Acraman impact displays feldspar- and fine-grained mica domains (Fig. 2A). The feldspar domain is composed of coarse-grained albite containing fine-grained, anhedral quartz inclusions, which are clasts of the Yardea Dacite, Gawler Ranges Volcanics. The fine-grained mica domain consists of elongated white-mica sheets, identified as muscovite through comparison of its EDS chemical composition with simulated data (Fig. 2B). In addition, fine-grained quartz, albite and ilmenite also occurs in minor abundance (Fig. 2C, D). The grain-size and polymineralic nature of the mica domain could have direct implication for in situ Rb–Sr dating, imposing limitations to date individual mica sheets (Fig. 2E). Nevertheless, fine-grained muscovite predominate in this texture, surpassing other minerals generally lack significant amounts of Rb and Sr, except for minor occurrences of very fine-grained feldspar. Thus, the Rb–Sr isotopic signal is likely to reflect the direct response of micas in such domain.

https://doi.org/10.5194/egusphere-2026-3441
Preprint. Discussion started: 25 June 2026
© Author(s) 2026. CC BY 4.0 License.

The Gosses Bluff melt-pellet features complex mineral textures with quartz-feldspar-mica intergrowth, and patches composed of ultrafine-grained mica targeted for in situ Rb–Sr geochronology (Fig. 3A). The ultrafine-grained micas are Fe-Mg-bearing classified as aliettite based on the comparison between its chemistry and simulated EDS composition (Fig. 3B). Simply, aliettite is a rare phyllosilicate linked to the dehydration of interstratified talc-trioctahedral smectite (Brigatti and Poppi, 1987), already reported in chondrites and impact-related settings (Bland et al., 2014). In high-spatial resolution backscatter images, the aliettite domains display extremely fine-grained, acicular micas with complex texture and potential chemical zoning (especially in Fe, Mg and Ca; major elements) with subordinate ilmenite (Fig. 3C). Some aliettite-bearing domains are sufficiently clear (i.e., monomineralic) to allow for individual laser spots (Fig. 3D). However, the intricate intergrowth with quartz-feldspar presents challenges in obtaining uncontaminated isotopic analyses, as it often results in mixing with a representative proportion of feldspar (Fig. 3E).

4.2. Single-collector triple quadrupole Rb–Sr geochronology

Muscovite from the Acraman sample yielded single Rb–Sr isochrons based on the data acquired by the Adelaide and Curtin University. We collected 46 Rb–Sr data at the Adelaide University, which yield an inverse isochron age of 562 ± 34 Ma (MSWD = 0.9) with an initial $^{87}Sr/^{86}Sr$ of 0.7279 ± 0.0074 (Fig. 4A). Overall, the individual $^{87}Rb/^{86}Sr$ ratios have an average internal uncertainty of 5.20 ± 2.80 % (standard deviation hereafter), and corresponding $^{87}Sr/^{86}Sr$ measurements with tighter average internal uncertainty of 1.99 ± 0.75 %. At 1'Curtin University, we collected 53 Rb–Sr data yielding an inverse isochron age of 584 ± 23 Ma (MSWD = 1.5) with an initial $^{87}Sr/^{86}Sr$ of 0.7189 ± 0.0067 (Fig. 4A). This dataset yielded more precise $^{87}Rb/^{86}Sr$ (2.67 ± 1.38 %) and $^{87}Sr/^{86}Sr$ (1.22 ± 0.55 %) likely due to the difference in laser parameters especially beam diameter.

The Rb–Sr data obtained at the Adelaide University of the aliettite domains from the Gosses Bluff melt-pellet yield average $^{87}Rb/^{86}Sr$ and $^{87}Sr/^{86}Sr$ internal uncertainty of 1.78 ± 1.32 % and

https://doi.org/10.5194/egusphere-2026-3441
Preprint. Discussion started: 25 June 2026
© Author(s) 2026. CC BY 4.0 License.

$^{87}Sr/^{86}Sr$ internal uncertainty of 1.13 ± 0.42 %. These data yield an isochron age of 91 ± 42 Ma (MSWD = 1.6, N = 56) with an initial $^{87}Sr/^{86}Sr$ of 0.7387 ± 0.0030 (Fig. 4C). We note some overdispersed data compared to the main isochron trend, and a high homogeneity in Rb/Sr ratio limiting the precision of the isochron age. The data obtained at Curtin University yielded comparatively less precise $^{87}Rb/^{86}Sr$ uncertainties (average of 3.74 ± 1.66 %; with some outliers with over 10 % internal uncertainty), but more precise $^{87}Sr/^{86}Sr$ (0.41 ± 0.17 %) compared to the Adelaide's dataset. The Curtin data yield an inverse isochron date of 169 ± 23 Ma (MSWD = 1.3) with an initial $^{87}Sr/^{86}Sr$ of 0.7174 ± 0.0004 (Fig. 4D).

4.3. Multi-collector Rb–Sr geochronology

The protocol utilized at Curtin University employing the ThermoFisher Neoma multi-collector yielded comparatively more precise isotopic ratios to the single-collector triple quadrupole protocol, yielding an overall internal $^{87}Rb/^{86}Sr$ precision of 3.66 ± 2.12 %, and significantly improved $^{87}Sr/^{86}Sr$ measurements (0.81 ± 0.30 %) compared to the single-collector triple quadrupole results. Across two analytical sessions, the Neoma data from the Acraman sample yielded the most precise isochron ages. The data collected in session 1 yielded an inverse isochron age of 575 ± 12 Ma (MSWD = 1.2, N = 42) with an initial $^{87}Sr/^{86}Sr$ of 0.7188 ± 0.0026, whereas the data collected in session 2 yielded an inverse isochron age of 588 ± 12 Ma (MSWD = 0.9, N = 40) with an initial $^{87}Sr/^{86}Sr$ 0.7187 ± 0.0023. Combined, the completed dataset yields an inverse isochron age of 580 ± 8 Ma (MSWD = 1.2, N = 82) with an initial $^{87}Sr/^{86}Sr$ of 0.7190 ± 0.0017, hereafter considered the most reliable and precise age for the Acraman ejecta layer.

The Gosses Bluff melt-pellet yielded complex Rb–Sr data dispersion due to the textural mixing between aliettite and feldspar (Fig. 3A, E). Data from the mixing spots (44 out of 73 from both sessions) are aligned with a reference isochron age of ca. 160 Ma, similar to the isochron age obtained from the Rb–Sr data obtained with Agilent 8900 at Curtin University (Fig. 4D). The Rb–Sr data from clean laser spots (i.e., with minimum feldspar mixing) yielded inverse isochron ages of 139 ± 14 Ma (MSWD = 1.2, N = 17; session 1) with initial $^{87}Sr/^{86}Sr$ of 0.7124 ± 0.0016 and 136

https://doi.org/10.5194/egusphere-2026-3441
Preprint. Discussion started: 25 June 2026
© Author(s) 2026. CC BY 4.0 License.

± 11 Ma (MSWD = 1.5, N = 12; session 2) with initial $^{87}Sr/^{86}Sr$ of 0.7236 ± 0.0015 (Fig. 5B). The complete dataset yields an inverse isochron age of 137 ± 9 Ma (MSWD = 1.6, N = 29) with initial $^{87}Sr/^{86}Sr$ of 0.7237 ± 0.0012, which we interpret as the best age estimate for the aliettite crystallization in the Gosses Bluff melt-pellet sample.

4.4. U–Pb geochronology

From the nine monazite U–Pb data we collected from the Acraman ejecta layer, only two are near-concordant yielding a weighted $^{206}Pb/^{238}U$ mean age of 980 ± 28 Ma (Fig. 6A). Fine-grained apatite texturally associated with the mica-bearing domain in the ejecta layer yield a lower intercept age in the Tera-Wasserburg of 1448 ± 79 Ma (MSWD = 2.0, N = 13; Fig. 6B) with an initial $^{207}Pb/^{206}Pb$ of 0.901 ± 0.0.029. Whilst both monazite and apatite yield distinctively older ages compared to the suggested Acraman impact age, fine-grained zircon embedded in the ejecta layer micaceous matrix yield a lower intercept age of 598 ± 16 Ma (MSWD = 0.5, N = 6; Fig. 6A) with an initial $^{207}Pb/^{206}Pb$ of 0.867 ± 0.016 as expected for the Neoproterozoic (Stacey and Kramers, 1975).

Zircon from the Gosses Bluff melt-pellet yield significantly overdispersed, discordant U–Pb data with only five near-concordant data smearing from ca. 1540 Ma down to ca. 510 Ma (Fig. 6C), imposing significantly limitation to constrain an impact age. Conversely, fine-grained apatite yield a well-defined mixing line between radiogenic and common-Pb components in Tera-Wasserburg space with a lower intercept age of 132 ± 14 Ma (MSWD = 0.4, N = 23; Fig. 6D) and initial $^{207}Pb/^{206}Pb$ of 0.856 ± 0.013 as expected for the Neoproterozoic (Stacey and Kramers, 1975).

5. Discussion

5.1. Comparison between in situ single- and multi-collector Rb–Sr geochronology

In situ Rb–Sr geochronology has been widely propelled by the new advances in mass spectrometers with collision-reaction cell that enable oxidizing reactions and consequently the measurement of ^{87}Rb-^{87}Sr interference-free (Cheng et al., 2008; Hogmalm et al., 2017; Redaa et

https://doi.org/10.5194/egusphere-2026-3441
Preprint. Discussion started: 25 June 2026
© Author(s) 2026. CC BY 4.0 License.

al., 2021a; Zack and Hogmalm, 2016). This includes single-collector triple quadrupole instruments including the Thermo Fisher iCap TQ and Agilent 8900, and the Thermo Fisher Neoma and NuPlasma Sapphire multi-collector mass spectrometers. Although single-collector triple quadrupole instruments have proven its ability to successfully date mica and feldspar from a range of rocks and textural settings (Li et al., 2020; Tillberg et al., 2020; Subarkah et al., 2022; Ribeiro et al., 2022, 2023b, 2023a, 2025; Liebmann et al., 2022; Zametzer et al., 2022; Kirkland et al., 2023; Larson et al., 2023; Almeida et al., 2023; Kellett et al., 2024; Nicomedes et al., 2025; Bedoya et al., 2025; Caxito et al., 2025, among many others), the development and optimization of analytical routines using multi-collector MS/MS instruments are still in its infancy (Bevan et al., 2021; Cruz-Uribe et al., 2023; Dauphas et al., 2022; Huang et al., 2025) – especially when referring to the comparison between those two instruments.

The protocols used at Curtin University employed identical laser parameters for Rb–Sr analyses with both the single-collector Agilent 8900 MS/MS and the multi-collector Thermo Fisher Neoma MS/MS, thereby enabling an independent comparison of instrument performance. Such comparison is often carried out using homogeneous materials (e.g., NIST SRM glasses), to exclude internal variability as a factor on measurement precision. As such, the Neoma MS/MS results yielded significantly more precise and accurate $^{87}Rb/^{86}Sr$ and $^{87}Sr/^{86}Sr$ ratios from NIST SRM 612 compared to the single-collector Agilent 8900 MS/MS (Fig. 7A), likely due to better performance of the Neoma MS/MS in measuring ^{84}SrF, ^{86}SrF and ^{87}SrF with high resistor Faraday cups of 10^{13} Ω (e.g., Huang et al., 2025) improving signal-to-noise ration and resulting in more precise isotopic measurements compared to the ion counter measurements in peak hoping mode on the Agilent 8900 triple quadrupole. This is more significant for minerals with high Sr concentration such as feldspar and some mica variations (e.g., white-mica and some biotite) (Bevan et al., 2021; Rankenburg et al., 2024), often yielding 10 times better internal precision on Sr isotopic measurements. For instance, we observed that Mount Dromedary biotite yielded more

https://doi.org/10.5194/egusphere-2026-3441
Preprint. Discussion started: 25 June 2026
© Author(s) 2026. CC BY 4.0 License.

precise $^{87}Rb/^{86}Sr$ (1.05 ± 0.50 %, internal precision) and $^{87}Sr/^{86}Sr$ (0.85 ± 0.20 %) ratios compared to Agilent 8900 ($^{87}Rb/^{86}Sr$ of 1.43 ± 0.27 %, and $^{87}Sr/^{86}Sr$ of 1.10 ± 0.17 %) (Fig. 7B, C). Conversely, low-Sr micas such as LaPosta biotite are better suited to be analyzed via ion-counted equipped instruments like the Agilent 8900 triple quadrupole, yielding more precise isotopic measurements compared to the Neoma MS/MS (Fig. 7B, C).

In summary, these results indicate that choosing the best analytical approach for unknown samples rely on knowing the estimated Sr concentration in the mineral of interest. Overall, the Neoma MS/MS is better suited to high-Sr, low Rb/Sr ratio specimens like alkali feldspar and some white-mica and clay mineral varieties (e.g., sericite, muscovite, illite and glauconite) (Bevan et al., 2021; Huang et al., 2025; Kirkland et al., 2025), resulting in tighter constrained isochron ages in spite of the narrow spread of $^{87}Rb/^{86}Sr$ ratios.

5.2. Assessing the chronology of the Acraman and Gosses Bluff impacts

The Acraman and Gosses Bluff impacts has been continuously investigated in respect to its potential significance with global climate and environmental events, requiring precise chronology to establish such correlations. Various dating approaches including whole-rock Rb–Sr (isotope dilution), whole-rock and minerals (e.g., feldspar) total fusion K-Ar and $^{40}Ar/^{39}Ar$, and zircon U–Pb and fission track have been applied to an array of impact-related samples including suevite and melt breccias (e.g., Jourdan, 2012; Milton et al., 1972; Milton and Sutter, 1987; Webb et al., 1983; Williams and Schmidt, 2021), but the impact age of the Acraman and Gosses Bluff remains debatable (Jourdan, 2012).

5.2.1. Acraman impact structure

Schmieder et al. (2015) carried out the latest and most comprehensive investigation of the Acraman chronology yet by focusing on U–Pb geochronology of unshocked and shocked zircon from impact-melt rocks and step-heating $^{40}Ar/^{39}Ar$ analysis of melted lithic dacite clasts and feldspar separates from shatter cones. Unshocked to moderately shocked zircon (with planar deformation features) from impact-melt rocks and from ejecta layers returned Mesoproterozoic

https://doi.org/10.5194/egusphere-2026-3441
Preprint. Discussion started: 25 June 2026
© Author(s) 2026. CC BY 4.0 License.

ages (c. 1.6 Ga) reflecting the magmatic age of the Gawler Volcanic Rages (Compston et al., 1987; Schmieder et al., 2015). ZrO_2-bearing granular zircon, often serving as gold-standard chronometer to constrain the timing of impact metamorphism (Erickson et al., 2021, 2020; Osinski et al., 2022; Timms et al., 2017), defined an ancient Pb-loss trend towards ca. 1114 Ma. Notably, this age is far from the Ediacaran ejecta-stratigraphic age bracket spanning 635–540 Ma considered the most reliable age interval for the timing of the Acraman impact, suggesting that granular zircon experienced partial diffusional Pb diffusion potentially attributed to impact metamorphism. Successive attempts in obtaining step-heating $^{40}Ar/^{39}Ar$ ages from impact-melt rocks and K-bearing mineral separates like alkali feldspar failed to yield plateau ages due to ^{39}Ar and ^{37}Ar recoil redistribution (Jourdan, 2012), or yielded (mini)-plateau ages younger than 460–450 Ma (Baldwin et al., 1991; Jourdan, 2012; Schmieder et al., 2015). Such young $^{40}Ar/^{39}Ar$ ages are interpreted to reflect post-impact hydrothermal alteration when compared to the ejecta-stratigraphic constraints, supported by the presented of secondary minerals (e.g., zeolite in vugs and chlorite and baryte in voids). To date, the ejecta layer whole-rock Rb–Sr isochron age of 588 ± 35 Ma may be considered the most reliable impact age (Webb et al., 1983), although its accuracy and statistical robustness are unknown.

Considering the Neoma superior precision for analysing the muscovite from the Acraman ejecta layer, the combined Neoma Rb–Sr isochron age of 580 ± 8 Ma is interpreted as the best age estimate for the Acraman impact. This age is supported by the new zircon U–Pb lower intercept age of 598 ± 16 Ma (although less precise) from the ejecta layer, and with the recent in situ Rb–Sr age of 585 ± 15 Ma from the Acraman ejecta layer obtained via single-collector triple quadrupole ICP-MS/MS (Collins et al., 2026). These results show that the known complications in dating the Acraman impact (e.g., inheritance or partial reset preserved in apatite and monazite and hydrothermal alteration as shown by the $^{40}Ar/^{30}Ar$ data) could be overcome through in situ laser beam techniques with sufficient lateral resolution to precisely date newly-grown mica

https://doi.org/10.5194/egusphere-2026-3441
Preprint. Discussion started: 25 June 2026
© Author(s) 2026. CC BY 4.0 License.

textures with more resilient isotopes to post-impact hydrothermal alteration and weathering such as Rb–Sr (and potentially K–Ca yet to be explored).

5.2.2. Gosses Bluff impact crater

Early investigations on the Gosses Bluff chronology have set an important framework to constraint the timing of meteorite impact directly using impact-related melt-rocks. Total fusion K–Ar dating of melt-rock (133 ± 3 Ma) and zircon fission track dating (134 ± 6 Ma) defined the best estimate for the timing of the Gosses Bluff impact (Milton et al., 1972; Milton and Sutter, 1987). Further attempts to refine this age with high-precision $^{40}Ar/^{39}Ar$ dating from pumiceous suevite clast and single sanidine grains from melt-rock yielded complex, discordant $^{39}Ar^{*}$ degassing patterns failing to yield plateau ages, rather displaying an increase age spectrum converging towards ca. 145 Ma (Jourdan, 2012; Milton and Sutter, 1987) (Fig. 8B). The older apparent age has been interpreted as minimum age for the Gosses Bluff impact (Jourdan, 2012).

In situ Rb–Sr data collected using single-collector triple quadrupole instruments did not produce accurate and precise ages, likely because of the complex feldspar-aliettite intergrowths (Fig. 3E) and the instrument's lower mass resolution compromising isotopic ratio precision and obscured variability arising from the textural complexity. The Neoma MS/MS yielded significantly more precise Sr isotopic measurements, allowing the distinction between isochrons defined by pure aliettite (137 ± 9 Ma) and mixing feldspar-aliettite domains (ca. 160 Ma; Fig. 5B). The younger isochron age from the pure aliettite domains is consistent with new apatite U–Pb lower intercept age of 132 ± 14 Ma, likely reflecting apatite growth from the impact melt, and with melt-rock K-Ar and zircon fission track ages (Milton et al., 1972; Milton and Sutter, 1987). Whilst the zircon from the Gosses Bluff melt-pellet yielded mostly discordant U–Pb data and an array of concordant data between 1540–510 Ma, potentially reflecting an inherited component or partial reset, preliminary results from granular, shock-recrystallized zircons suggest mean U–Pb age of 139 ± 4 Ma (Cousins et al., 2025).

https://doi.org/10.5194/egusphere-2026-3441
Preprint. Discussion started: 25 June 2026
© Author(s) 2026. CC BY 4.0 License.

Collectively, the published and new ages (this study) from the Gosses Bluff points to an impact age of 133 ± 3 Ma (Fig. 8B), indicating that older $^{40}Ar/^{39}Ar$ data with complex degassing spectra could represent excess and/or inherited $^{40}Ar^{*}$ likely producing older apparent ages (e.g., Jourdan et al., 2007).

5.3. Advances and limitations of in situ mica Rb–Sr geochronology in meteorite impacts

In situ mica Rb–Sr geochronology has been successfully applied to dating complex textures in deformed rocks (e.g, Kirkland et al., 2023; Larson et al., 2023; Ribeiro et al., 2023a, 2023b; Tollefson and Larson, 2026; Tollefson et al., 2025), yet the behavior of Rb–Sr isotopes in shocked micas and its potential to constraint the timing of impact processes remain underexplored (Ribeiro et al., 2026).

The Rb–Sr results from the Acraman and Gosses Bluff impacts have shown newly grown micas in ejecta layer and melt-rocks have the potential to preserve the timing of impact processes, whilst apparently less susceptible to post-impact hydrothermal alteration compared to Ar isotopes (Jourdan, 2012; Milton and Sutter, 1987). Additionally, the lateral-spatial resolution achieved by modern laser ablation system provide the means to resolve complex textural relationships, intrinsic to impact-related rocks, aid in obtaining clean analytical data. Combined with high-precision reaction-cell instruments, such as the Thermo Fisher Neoma multi-collector, in situ Rb–Sr dating of complex mica textures can overcome challenges posed by inherited or altered isotopic systems and obtain chronologies that more accurately reflect the timing of meteorite impacts such as inherited and/or excess 40Ar* (Jourdan, 2012; Jourdan et al., 2007). Since micas are widely abundant on terrestrial rocks (Bailey, 1984), in situ Rb–Sr also circumvents the challenges of dating accessory phases (< 1 vol.%) such as apatite, zircon and monazite. Despite being powerful to precisely define the timing of impact via U–Pb system in some cases (Erickson et al., 2021, 2020; Kenny et al., 2019; Kirkland et al., 2025), those accessory minerals often yield complex datasets due to inheritance components and/or partial isotopic resetting as observed in this study and in many other impact sites (Bohor et al., 1993; Erickson et al., 2021, 2017; Kirkland

https://doi.org/10.5194/egusphere-2026-3441
Preprint. Discussion started: 25 June 2026
© Author(s) 2026. CC BY 4.0 License.

et al., 2025; McGregor et al., 2019; Ribeiro et al., 2026; Schmieder et al., 2015). In such cases, newly grown micas not only are far more abundant and easier to date via in situ Rb–Sr techniques, but it can also provide high-quality isotopic data to pinpoint the timing of impact processes at relevant precision. As this field advances, the reliability and applicability of in situ Rb–Sr geochronology may provide valuable insights into both terrestrial and planetary impact events (e.g., Luu et al., 2026).

Despite these encouraging new results, in situ Rb–Sr results of pre-impact micas from the Yarrabubba impact structure has shown that these isotopes are resilient to impact-driven resetting despite the formation of shock-related microstructures that could enhance isotope diffusion (Ribeiro et al., 2026). Yet they preserve the protolith's crystallization age rather than the impact age, likely due to the short timescale of the thermal peak phase associated with impact metamorphism (Ribeiro et al., 2026). We recommend that future mica dating studies on impact-related rocks focus on newly grown textures, as they are more likely to provide accurate impact ages.

5.4. Further applications for in situ Rb–Sr dating in planetary sciences

K-bearing minerals including alkali feldspar and a wide variety of micas (white-mica, biotite, phlogopite) and clays (illite-smectite) are common on Earth's terrestrial rocks, but also on extraterrestrial rocks (Foland, 1998). In addition to being datable via K-Ar, $^{40}Ar/^{39}Ar$, they are also potential targets for in situ Rb–Sr dating opening a new research avenue to investigate impact-melt formation, deformation and syn- to post-impact hydrothermal alteration on Earth and extraterrestrial materials (e.g., Papanastassiou and Wasserburg, 1972a, 1972b). The use of Rb–Sr isotopes, chemically separated via isotope dilution and independently measured in solution mode, has been successfully employed to explore the timing and nature of aqueous alteration of Martian meteorites (Beard et al., 2013), defining the time and duration of lunar crust formation (Carlson et al., 2014) and the overall isotopic evolution of Martian meteorites in combination with other radiogenic isotopes (Borg et al., 2005).

https://doi.org/10.5194/egusphere-2026-3441
Preprint. Discussion started: 25 June 2026
© Author(s) 2026. CC BY 4.0 License.

Although isotope dilution Rb–Sr isotopic measurements provide precise isotopic ratios from critical, but low-abundance Rb and Sr minerals encountered in extraterrestrial rocks including orthopyroxene, plagioclase and chromite (e.g., Papanastassiou and Wasserburg, 1972b; Beard et al., 2013), the development and optimization of in situ Rb–Sr analysis isotopic measurements via multi-collector ICP-MS/MS holds significant promise for exploring extraterrestrial materials with accessible, speedy, low-cost technique (Dauphas et al., 2022; Nie et al., 2024). The capability to target specific mineral phases could provide critical insights into the timing of planetary surface evolution, the chronology of impact events across the solar system, and the associated effects on planetary environments and potential habitability. As analytical techniques continue to improve, in situ Rb–Sr geochronology is poised to become a valuable tool for unraveling complex geological histories both on Earth and beyond.

6. Conclusions

This study demonstrates the significant advances and ongoing challenges of in situ Rb–Sr geochronology for precisely dating impact-related processes in both terrestrial and extraterrestrial materials. Newly grown micas in ejecta layers and melt-rocks have proven to be robust recorders of meteorite impact timing, offering greater resistance to post-impact alteration compared to traditional Ar isotope systems. Modern analytical techniques, including high-resolution laser ablation and multi-collector mass spectrometry, enable the resolution of complex mineral textures and improve the accuracy of isotopic measurements. The resilience of pre-impact micas to isotopic resetting highlights the importance of targeting newly formed mineral domains for reliable age determinations. Further, the application of in situ Rb–Sr dating to planetary science opens new avenues for understanding planetary surface evolution, impact histories, and related hydrothermal processes. As analytical methods continue to evolve, in situ Rb–Sr geochronology is poised to provide critical insights into the timing and effects of impact events across our solar system.

https://doi.org/10.5194/egusphere-2026-3441
Preprint. Discussion started: 25 June 2026
© Author(s) 2026. CC BY 4.0 License.

Acknowledgements

This work is supported by the Timescales of Mineral Systems Group (Curtin University). Instruments in the John de Laeter Centre, Curtin University, are supported by the Australian Research Council, AuScope, and the Australian Government via the National Collaborative Research Infrastructure Strategy. This research was undertaken using the Tescan Clara FESEM (ARC LE190100176) at the John de Laeter Centre, Curtin University.

Author's contributions

Bruno V. Ribeiro: Conceptualization, formal analysis, data curation, writing – original draft
Jayden Squire: Conceptualization, formal analysis, data curation, writing – original draft
Christopher Kirkland: Conceptualization, validation, writing – original draft
Juraj Farkas: Conceptualization, validation, writing – original draft
Cecilia Loyola: Formal analysis, data curation, writing – review and editing
Victoria Cousins: Formal analysis, data curation, writing – review and editing
Victor Gostin: Validation, writing – review and editing
Charles Verdel: Validation, writing – review and editing

Competing interests

Authors declare that they have no competing interests.

https://doi.org/10.5194/egusphere-2026-3441
Preprint. Discussion started: 25 June 2026
© Author(s) 2026. CC BY 4.0 License.

References

Aleinikoff, J.N., Schenck, W.S., Plank, M.O., Srogi, L., Fanning, C.M., Kamo, S.L., Bosbyshell, H., 2006. Deciphering igneous and metamorphic events in high-grade rocks of the Wilmington Complex, Delaware: Morphology, cathodoluminescence and backscattered electron zoning, and SHRIMP U-Pb geochronology of zircon and monazite. Geol. Soc. Am. Bull. 118, 39–64.

Almeida, V.V., Ribeiro, B.V., Rodrigues, J.B., Cawood, P.A., Neto, I.C., Silveira, F.V., Faleiros, F.M., Kirscher, U., 2023. Linking kimberlite magmatism in the Brazilian Platform with Pangea break-up events using in situ Rb Sr in phlogopite. Lithos 107486. https://doi.org/10.1016/j.lithos.2023.107486

Apen, F.E., Gaynor, S.P., Schoene, B., Cottle, J.M., 2024. Evaluating reference materials and common-Pb corrections for high-resolution apatite U Pb geochronology. Chem. Geol. 661, 122191. https://doi.org/10.1016/j.chemgeo.2024.122191

Artemieva, N., Morgan, J., 2017. Quantifying the Release of Climate-Active Gases by Large Meteorite Impacts With a Case Study of Chicxulub. Geophys. Res. Lett. 44. https://doi.org/10.1002/2017GL074879

Bailey, S.W., 1984. Micas: Reviews in Mineralogy . Mineralogical Society of America.

Baldwin, S.L., McDougall, I., Williams, G.E., 1991. K/Ar and 40Ar/39Ar analyses of meltrock from the Acraman impact structure, Gawler Ranges, South Australia. Australian Journal of Earth Sciences 38, 291–298. https://doi.org/10.1080/08120099108727973

Beard, B.L., Ludois, J.M., Lapen, T.J., Johnson, C.M., 2013. Pre-4.0 billion year weathering on Mars constrained by Rb–Sr geochronology on meteorite ALH84001. Earth Planet. Sci. Lett. 361, 173–182. https://doi.org/10.1016/j.epsl.2012.10.021

Bedoya, A., Glorie, S., Hand, M., Kirkland, C.L., De Vries Van Leeuwen, A.T., 2025. In situ Rb–Sr insights in the cooling history of the Petermann Orogeny, Central Australia. Geoscience Frontiers 16, 102080. https://doi.org/10.1016/j.gsf.2025.102080

Bevan, D., Coath, C.D., Lewis, J., Schwieters, J., Lloyd, N., Craig, G., Wehrs, H., Elliott, T., 2021. In situ Rb–Sr dating by collision cell, multicollection inductively-coupled plasma mass-spectrometry with pre-cell mass-filter, (CC-MC-ICPMS/MS). J. Anal. At. Spectrom. 36, 917–931. https://doi.org/10.1039/D1JA00006C

Bland, P.A., Collins, G.S., Davison, T.M., Abreu, N.M., Ciesla, F.J., Muxworthy, A.R., Moore, J., 2014. Pressure–temperature evolution of primordial solar system solids during impact-induced compaction. Nat. Commun. 5, 5451. https://doi.org/10.1038/ncomms6451

Bohor, B.F., Betterton, W.J., Krogh, T.E., 1993. Impact-shocked zircons: discovery of shock-induced textures reflecting increasing degrees of shock metamorphism. Earth Planet. Sci. Lett. 119, 419–424. https://doi.org/10.1016/0012-821X(93)90149-4

Borg, L.E., Edmunson, J.E., Asmerom, Y., 2005. Constraints on the U-Pb isotopic systematics of Mars inferred from a combined U-Pb, Rb-Sr, and Sm-Nd isotopic study of the Martian meteorite Zagami. Geochim. Cosmochim. Acta 69, 5819–5830. https://doi.org/10.1016/j.gca.2005.08.007

Brigatti, M.F., Poppi, L., 1987. Natural and monoionic aliettite: hydration and dehydration states. Clay Miner. 22, 187–197. https://doi.org/10.1180/claymin.1987.022.2.07

https://doi.org/10.5194/egusphere-2026-3441
Preprint. Discussion started: 25 June 2026
© Author(s) 2026. CC BY 4.0 License.

559 Carlson, R.W., Borg, L.E., Gaffney, A.M., Boyet, M., 2014. Rb-Sr, Sm-Nd and Lu-Hf isotope systematics of
560 the lunar Mg-suite: the age of the lunar crust and its relation to the time of Moon formation.
561 Philosophical Transactions of the Royal Society A: Mathematical, Physical and Engineering Sciences
562 372, 20130246. https://doi.org/10.1098/rsta.2013.0246
563 Caxito, F.A., Ribeiro, B. V., Alkmim, F., Deramchi, A., Kirkland, C.L., 2025. Near-Synchronous Cambrian
564 Evolution of the Transbrasiliano-Kandi-4°50' Shear Zone in South America and Africa. Terra Nova.
565 https://doi.org/10.1111/ter.70017
566 Cheng, P., Koyanagi, G.K., Bohme, D.K., 2008. On the chemical resolution of the 87Rb+ (s0)/87Sr+ (s1)
567 isobaric interference: A kinetic search for an optimum reagent. Anal. Chim. Acta 627, 148–153.
568 https://doi.org/10.1016/j.aca.2008.03.057
569 Cockell, C.S., Lee, P., Osinski, G., Horneck, G., Broady, P., 2002. Impact-induced microbial endolithic
570 habitats. Meteorit. Planet. Sci. 37, 1287–1298. https://doi.org/10.1111/j.1945-
571 5100.2002.tb01029.x
572 Collins, A.S., Blades, M.L., Subarkah, D., Cooke, H., Edwards, L., Forbister, C., Jolly, J., Lloyd, J.C., Gilbert,
573 S.E., Löhr, S., Farkaš, J., Gostin, V., 2026. Age of the Acraman impact ejecta layer in the adelaide
574 superbasin and Implications on clay-mineral provenance from the Rb–Sr systematics of middle
575 Ediacaran shales. Precambrian Res. 435, 108015.
576 https://doi.org/10.1016/j.precamres.2026.108015
577 Collins, G.S., Melosh, H.J., Osinski, G.R., 2012. The Impact-Cratering Process. Elements 8, 25–30.
578 https://doi.org/10.2113/gselements.8.1.25
579 Compston, W., Williams, I.S., Jenkins, R.J.F., Gostin, V.A., Haines, P.W., 1987. Zircon age evidence for the
580 Late Precambrian Acraman ejecta blanket. Australian Journal of Earth Sciences 34, 435–445.
581 https://doi.org/10.1080/08120098708729424
582 Cousins, V.K., Cavosie, A.J., Timms, N.E., Quintero, R.R., Kirkland, C.L., Evans, N.J., McDonald, B., 2025.
583 Constraining the Age of Impact: A Microstructural Investigation of Zircon from the Gosses Bluff
584 Impact Structure, Australia, in: 87th Annual Meeting of the Meteoritical Society. Perth, Western
585 Australia.
586 Crook, K.A.W., Cook, P.J., 1966. Gosses bluff — diapir, crypto-volcanic structure or astrobleme?∗. Journal
587 of the Geological Society of Australia 13, 495–516. https://doi.org/10.1080/00167616608728628
588 Cruz-Uribe, A.M., Craig, G., Garber, J.M., Paul, B., Arkula, C., Bouman, C., 2023. Single Spot Rb-Sr
589 Isochron Dating of Biotite by LA-MC-ICP-MS/MS. Geostand. Geoanal. Res. 47, 795–809.
590 https://doi.org/10.1111/ggr.12518
591 Dauphas, N., Hopp, T., Craig, G., Zhang, Z.J., Valdes, M.C., Heck, P.R., Charlier, B.L.A., Bell, E.A., Harrison,
592 T.M., Davis, A.M., Dussubieux, L., Williams, P.R., Krawczynski, M.J., Bouman, C., Lloyd, N.S.,
593 Tollstrup, D., Schwieters, J.B., 2022. In situ 87Rb–87Sr analyses of terrestrial and extraterrestrial
594 samples by LA-MC-ICP-MS/MS with double Wien filter and collision cell technologies. J. Anal. At.
595 Spectrom. 37, 2420–2441. https://doi.org/10.1039/D2JA00135G
596 Dietz, R.S., 1967. Shatter Cone Orientation at Gosses Bluff Astrobleme. Nature 216, 1082–1084.
597 https://doi.org/10.1038/2161082a0
598 Erickson, T.M., Kirkland, C.L., Jourdan, F., Schmieder, M., Hartnady, M.I.H., Cox, M.A., Timms, N.E., 2021.
599 Resolving the age of the Haughton impact structure using coupled 40Ar/39Ar and U-Pb
600 geochronology. Geochim. Cosmochim. Acta 304, 68–82. https://doi.org/10.1016/j.gca.2021.04.008

https://doi.org/10.5194/egusphere-2026-3441
Preprint. Discussion started: 25 June 2026
© Author(s) 2026. CC BY 4.0 License.

Erickson, T.M., Kirkland, C.L., Timms, N.E., Cavosie, A.J., Davison, T.M., 2020. Precise radiometric age establishes Yarrabubba, Western Australia, as Earth's oldest recognised meteorite impact structure. Nat. Commun. 11, 300. https://doi.org/10.1038/s41467-019-13985-7

Erickson, T.M., Timms, N.E., Kirkland, C.L., Tohver, E., Cavosie, A.J., Pearce, M.A., Reddy, S.M., 2017. Shocked monazite chronometry: integrating microstructural and in situ isotopic age data for determining precise impact ages. Contributions to Mineralogy and Petrology 172, 11. https://doi.org/10.1007/s00410-017-1328-2

Foland, K.A., 1998. Potassium-argon dating method, in: Geochemistry. Kluwer Academic Publishers, Dordrecht, pp. 522–525. https://doi.org/10.1007/1-4020-4496-8_259

French, B.M., Koeberl, C., 2010. The convincing identification of terrestrial meteorite impact structures: What works, what doesn't, and why. Earth. Sci. Rev. 98, 123–170. https://doi.org/10.1016/j.earscirev.2009.10.009

Giuliani, A., Oesch, S., Guillong, M., Howarth, G.H., 2024. Mica Rb-Sr dating by laser ablation ICP-MS/MS using an isochronous calibration material and application to West African kimberlites. Chem. Geol. 649, 121982. https://doi.org/10.1016/j.chemgeo.2024.121982

Gostin, V.A., Haines, P.W., Jenkins, R.J.F., Compston, W., Williams, I.S., 1986. Impact Ejecta Horizon Within Late Precambrian Shales, Adelaide Geosyncline, South Australia. Science (1979). 233, 198–200. https://doi.org/10.1126/science.233.4760.198

Guerrero, D., Reimold, W.U., Hauser, N., Kenny, G., Whitehouse, M., Lambert, P., 2025. Shock deformation and U-Pb isotope systematics in zircon from impactites of the Rochechouart impact structure: Impact age and zircon provenance. Geochim. Cosmochim. Acta 402, 338–358. https://doi.org/10.1016/j.gca.2025.05.049

Hayward, C.L., Reimold, W.U., Gibson, R.L., Robb, L.J., 2005. Gold mineralization within the Witwatersrand Basin, South Africa: evidence for a modified placer origin, and the role of the Vredefort impact event. Geological Society, London, Special Publications 248, 31–58. https://doi.org/10.1144/GSL.SP.2005.248.01.02

Herrmann, M., Kenny, G.G., Martell, J., Whitehouse, M.J., Alwmark, C., 2024. The first U–Pb age for shocked zircon from the Mien impact structure, Sweden, and implications for metamictization-induced zircon texture formed during impact events. Meteorit. Planet. Sci. 59, 211–241. https://doi.org/10.1111/maps.14116

Hildebrand, A.R., Penfield, G.T., Kring, D.A., Pilkington, M., Camargo Z., A., Jacobsen, S.B., Boynton, W. V., 1991. Chicxulub Crater: A possible Cretaceous/Tertiary boundary impact crater on the Yucatán Peninsula, Mexico. Geology 19, 867. https://doi.org/10.1130/0091-7613(1991)019<0867:CCAPCT>2.3.CO;2

Hill, A.C., Haines, P.W., Grey, K., Willman, S., 2007. New records of Ediacaran Acraman ejecta in drillholes from the Stuart Shelf and Officer Basin, South Australia. Meteorit. Planet. Sci. 42, 1883–1891. https://doi.org/10.1111/j.1945-5100.2007.tb00547.x

Hogmalm, K.J., Zack, T., Karlsson, A.K., Sjoqvist, A.S.L., Grabe-Schonberg, D., 2017. In-situ Rb-Sr and K-Ca dating by LA-ICP-MS/MS: An evaluation of N2O and SF6 as reaction gases. J. Anal. At. Spectrom. 32, 305–313.

Horstwood, M.S.A., Košler, J., Gehrels, G., Jackson, S.E., McLean, N.M., Paton, C., Pearson, N.J., Sircombe, K., Sylvester, P., Vermeesch, P., Bowring, J.F., Condon, D.J., Schoene, B., 2016.

https://doi.org/10.5194/egusphere-2026-3441
Preprint. Discussion started: 25 June 2026
© Author(s) 2026. CC BY 4.0 License.

Community-Derived Standards for LA-ICP-MS U-(Th-)Pb Geochronology – Uncertainty Propagation, Age Interpretation and Data Reporting. Geostand. Geoanal. Res. 40, 311–332. https://doi.org/10.1111/j.1751-908X.2016.00379.x

Hrstka, T., Gottlieb, P., Skála, R., Breiter, K., Motl, D., 2018. Automated mineralogy and petrology - applications of TESCAN Integrated Mineral Analyzer (TIMA). Journal of Geosciences 47–63. https://doi.org/10.3190/jgeosci.250

Hu, Z., Gao, S., Liu, Y., Hu, S., Chen, H., Yuan, H., 2008. Signal enhancement in laser ablation ICP-MS by addition of nitrogen in the central channel gas. J. Anal. At. Spectrom. 23, 1093. https://doi.org/10.1039/b804760j

Huang, C., Wang, H., Xie, L., Xu, L., Wu, S., Yang, Y., Yang, J., 2025. High-precision Rb-Sr isotope analysis with Neoma MS/MS: Enhancing in situ geochronology by laser ablation. Spectrochim. Acta Part B At. Spectrosc. 224, 107117. https://doi.org/10.1016/j.sab.2025.107117

Jackson, S.E., Pearson, N.J., Griffin, W.L., Belousova, E.A., 2004. The application of laser ablation-inductively coupled plasma-mass spectrometry to in situ U–Pb zircon geochronology. Chem. Geol. 211, 47–69.

Jourdan, F., 2012. The 40Ar/39Ar dating technique applied to planetary sciences and terrestrial impacts. Australian Journal of Earth Sciences 59, 199–224. https://doi.org/10.1080/08120099.2012.644404

Jourdan, F., Reimold, W.U., Deutsch, A., 2012. Dating Terrestrial Impact Structures. Elements 8, 49–53. https://doi.org/10.2113/gselements.8.1.49

Jourdan, F., Renne, P.R., Reimold, W.U., 2009. An appraisal of the ages of terrestrial impact structures. Earth Planet. Sci. Lett. 286, 1–13. https://doi.org/10.1016/j.epsl.2009.07.009

Jourdan, F., Renne, P.R., Reimold, W.U., 2007. The problem of inherited 40Ar* in dating impact glass by the 40Ar/39Ar method: Evidence from the Tswaing impact crater (South Africa). Geochim. Cosmochim. Acta 71, 1214–1231. https://doi.org/10.1016/j.gca.2006.11.013

Kellett, D.A., Larson, K.P., Skipton, D.R., 2024. Integration of white mica in situ 87Rb/87Sr with in situ and step-heat 40Ar/39Ar dates in orogenic settings. Lithos 482–483, 107687. https://doi.org/10.1016/j.lithos.2024.107687

Kenny, G.G., Schmieder, M., Whitehouse, M.J., Nemchin, A.A., Morales, L.F.G., Buchner, E., Bellucci, J.J., Snape, J.F., 2019. A new U-Pb age for shock-recrystallised zircon from the Lappajärvi impact crater, Finland, and implications for the accurate dating of impact events. Geochim. Cosmochim. Acta 245, 479–494. https://doi.org/10.1016/j.gca.2018.11.021

Kirkland, C.L., Erickson, T.M., Johnson, T.E., Prave, T., Strachan, R.A., Daggitt, M.L., Hartnady, M.I.H., Reddy, S.M., Taylor, R.J.M., Ribeiro, B.V., Rankenburg, K., Kirscher, U., Fischer, S., 2025. A one-billion-year-old Scottish meteorite impact. Geology 53, 621–625. https://doi.org/10.1130/G53121.1

Kirkland, C.L., Olierook, H.K.H., Danišík, M., Liebmann, J., Hollis, J., Ribeiro, B. V., Rankenburg, K., 2023. Dating mylonitic overprinting of ancient rocks. Commun. Earth Environ. 4, 47. https://doi.org/10.1038/s43247-023-00709-5

Larson, K.P., Button, M., Shrestha, S., Camacho, A., 2023. A comparison of 87Rb/87Sr and 40Ar/39Ar dates: Evaluating the problem of excess 40Ar in Himalayan mica. Earth Planet. Sci. Lett. 609, 118058. https://doi.org/10.1016/j.epsl.2023.118058

https://doi.org/10.5194/egusphere-2026-3441
Preprint. Discussion started: 25 June 2026
© Author(s) 2026. CC BY 4.0 License.

Li, S.S., Santosh, M., Farkaš, J., Redaa, A., Ganguly, S., Kim, S.W., Zhang, C., Gilbert, S., Zack, T., 2020. Coupled U-Pb and Rb-Sr laser ablation geochronology trace Archean to Proterozoic crustal evolution in the Dharwar Craton, India. Precambrian Res. 343. https://doi.org/10.1016/j.precamres.2020.105709

Liebmann, J., Kirkland, C.L., Kelsey, D.E., Korhonen, F.J., Rankenburg, K., 2022. Lithological fabric as a proxy for Rb–Sr isotopic complexity. Chem. Geol. 608, 121041. https://doi.org/10.1016/j.chemgeo.2022.121041

Luu, T.-H., Peters, D., Gérard, Y., Crawshaw, H., Moynier, F., 2026. Precise in situ 87Rb-87Sr dating of terrestrial and extraterrestrial samples with Nu Sapphire XD LA-CRC-MC-ICP-MS/MS. J. Anal. At. Spectrom. https://doi.org/10.1039/D6JA00061D

McCall, G.J.H., 2006. The Vendian (Ediacaran) in the geological record: Enigmas in geology's prelude to the Cambrian explosion. Earth. Sci. Rev. 77, 1–229. https://doi.org/10.1016/j.earscirev.2005.08.004

McGregor, M., McFarlane, C.R.M., Spray, J.G., 2019. In situ multiphase U–Pb geochronology and shock analysis of apatite, titanite and zircon from the Lac La Moinerie impact structure, Canada. Contributions to Mineralogy and Petrology 174, 62. https://doi.org/10.1007/s00410-019-1598-y

Milton, D.J., Glikson, A.Y., Manwaring, E.A., Moss, F.J., Sedmik, E.C.E., Van Son, J., Barlow, B.C., Brett, R., Young, G.A., 1972. Gosses Bluff Impact Structure, Australia. Science (1979). 175, 1199–1207. https://doi.org/10.1126/science.175.4027.1199

Milton, D.J., Sutter, J.F., 1987. Revised age for the Gosses Bluff impact structure, Northern Territory, Australia, based on 40Ar/39Ar dating. Meteoritics 22, 281–289. https://doi.org/10.1111/j.1945-5100.1987.tb00625.x

Montel, J.-M., Foret, S., Veschambre, M., Nicollet, C., Provost, A., 1996. Electron microprobe dating of monazite. Chem. Geol. 131, 37–53. https://doi.org/10.1016/0009-2541(96)00024-1

Nicomedes, I.S., Ribeiro, B. V., Caxito, F.A., Kirkland, C.L., Victoria, A., Quadir, Z., 2025. In situ Rb–Sr geochronology of slickensides reveals reactivation of cratonic margins post-Gondwana assembly. J. Struct. Geol. 191, 105305. https://doi.org/10.1016/j.jsg.2024.105305

Nie, N.X., Dauphas, N., Zhang, Z.J., Hopp, T., Sarantos, M., 2024. Lunar soil record of atmosphere loss over eons. Sci. Adv. 10. https://doi.org/10.1126/sciadv.adm7074

Osinski, G.R., Cockell, C.S., Pontefract, A., Sapers, H.M., 2020. The Role of Meteorite Impacts in the Origin of Life. Astrobiology 20, 1121–1149. https://doi.org/10.1089/ast.2019.2203

Osinski, G.R., Grieve, R.A.F., Ferrière, L., Losiak, A., Pickersgill, A.E., Cavosie, A.J., Hibbard, S.M., Hill, P.J.A., Bermudez, J.J., Marion, C.L., Newman, J.D., Simpson, S.L., 2022. Impact Earth: A review of the terrestrial impact record. Earth. Sci. Rev. 232, 104112. https://doi.org/10.1016/j.earscirev.2022.104112

Papanastassiou, D.A., Wasserburg, G.J., 1972a. The Rb-Sr age of a crystalline rock from Apollo 16. Earth Planet. Sci. Lett. 16, 289–298. https://doi.org/10.1016/0012-821X(72)90205-1

Papanastassiou, D.A., Wasserburg, G.J., 1972b. Rb-Sr age of a Luna 16 basalt and the model age of lunar soils. Earth Planet. Sci. Lett. 13, 368–374. https://doi.org/10.1016/0012-821X(72)90111-2

Paton, C., Hellstrom, J., Paul, B., Woodhead, J., Hergt, J., 2011a. Iolite: Freeware for the visualisation and processing of mass spectrometric data. J. Anal. At. Spectrom. 26, 2508. https://doi.org/10.1039/c1ja10172b

https://doi.org/10.5194/egusphere-2026-3441
Preprint. Discussion started: 25 June 2026
© Author(s) 2026. CC BY 4.0 License.

Paton, C., Hellstrom, J., Paul, B., Woodhead, J., Hergt, J., 2011b. Iolite: Freeware for the visualisation and processing of mass spectrometric data. J. Anal. At. Spectrom. 26, 2508–2518.

Quintero, R.R., Cavosie, A.J., Cox, M.A., Miljković, K., Dugdale, A., 2021. Australian impact cratering record: Updates and recent discoveries, in: Large Meteorite Impacts and Planetary Evolution VI. Geological Society of America, pp. 41–68. https://doi.org/10.1130/2021.2550(02)

Rankenburg, K., Ribeiro, B.V., Evans, N.J., McDonald, B., 2024. Comparing CRC-MC-ICPMS to QQQ-ICPMS/MS for in situ Rb-Sr applications, in: Goldschmidt. Chicago.

Redaa, A., Farkaš, J., Gilbert, S., Collins, A.S., Wade, B., Löhr, S., Zack, T., Garbe-Schönberg, D., 2021a. Assessment of elemental fractionation and matrix effects during *in situ* Rb–Sr dating of phlogopite by LA-ICP-MS/MS: implications for the accuracy and precision of mineral ages. J. Anal. At. Spectrom. 36, 322–344. https://doi.org/10.1039/D0JA00299B

Redaa, A., Farkaš, J., Gilbert, S., Collins, A.S., Wade, B., Löhr, S., Zack, T., Garbe-Schönberg, D., 2021b. Assessment of elemental fractionation and matrix effects during *in situ* Rb–Sr dating of phlogopite by LA-ICP-MS/MS: implications for the accuracy and precision of mineral ages. J. Anal. At. Spectrom. 36, 322–344. https://doi.org/10.1039/D0JA00299B

Reimold, W.U., Koeberl, C., Gibson, R.L., Dressler, B.O., 2005. Economic Mineral Deposits in Impact Structures: A Review. Impact Tectonics 479–552. https://doi.org/10.1007/3-540-27548-7_20

Ribeiro, B.V., Finch, M.A., Cawood, P.A., Faleiros, F.M., Murphy, T.D., Simpson, A., Glorie, S., Tedeschi, M., Armit, R., Barrote, V.R., 2022. From microanalysis to supercontinents: Insights from the Rio Apa Terrane into the Mesoproterozoic SW Amazonian Craton evolution during Rodinia assembly. Journal of Metamorphic Geology 40, 631–663. https://doi.org/10.1111/jmg.12641

Ribeiro, B.V., Jakobsson, V., Kirkland, C.L., Spikings, R.A., Zametzer, A., Rickard, W.D.A., Centrella, S., Timms, N.E., Cavosie, A.J., Danišík, M., 2026. Microstructural and geochemical response of muscovite to impact metamorphism. Geology 54, 179–183. https://doi.org/10.1130/G53895.1

Ribeiro, B. V., Kirkland, C.L., Finch, M.A., Faleiros, F.M., Reddy, S.M., Rickard, W.D.A., Hartnady, M.I.H., 2023a. Microstructures, geochemistry, and geochronology of mica fish: Review and advances. J. Struct. Geol. 104947. https://doi.org/10.1016/j.jsg.2023.104947

Ribeiro, B. V., Kirkland, C.L., Kelsey, D.E., Reddy, S.M., Hartnady, M.I.H., Faleiros, F.M., Rankenburg, K., Liebmann, J., Korhonen, F.J., Clark, C., 2023b. Time-strain evolution of shear zones from petrographically constrained Rb–Sr muscovite analysis. Earth Planet. Sci. Lett. 602, 117969. https://doi.org/10.1016/j.epsl.2022.117969

Rösel, D., Zack, T., 2022. LA-ICP-MS/MS Single-Spot Rb-Sr Dating. Geostand. Geoanal. Res. https://doi.org/10.1111/ggr.12414

Schmieder, M., Tohver, E., Jourdan, F., Denyszyn, S.W., Haines, P.W., 2015. Zircons from the Acraman impact melt rock (South Australia): Shock metamorphism, U–Pb and 40 Ar/ 39 Ar systematics, and implications for the isotopic dating of impact events. Geochim. Cosmochim. Acta 161, 71–100. https://doi.org/10.1016/j.gca.2015.04.021

Schmitz, M.D., Bowring, S.A., Ireland, T.R., 2003. Evaluation of Duluth Complex anorthositic series (AS3) zircon as a U-Pb geochronological standard: new high-precision isotope dilution thermal ionization mass spectrometry results. Geochim. Cosmochim. Acta 67, 3665–3672. https://doi.org/10.1016/S0016-7037(03)00200-X

https://doi.org/10.5194/egusphere-2026-3441
Preprint. Discussion started: 25 June 2026
© Author(s) 2026. CC BY 4.0 License.

Schoene, B., Bowring, S.A., 2006. U-Pb systematics of the McClure Mountain syenite: Thermochronological constraints on the age of the 40Ar/39Ar standard MMhb. Contributions to Mineralogy and Petrology 151, 615–630. https://doi.org/10.1007/s00410-006-0077-4

Schulte, P., Alegret, L., Arenillas, I., Arz, J.A., Barton, P.J., Bown, P.R., Bralower, T.J., Christeson, G.L., Claeys, P., Cockell, C.S., Collins, G.S., Deutsch, A., Goldin, T.J., Goto, K., Grajales-Nishimura, J.M., Grieve, R.A.F., Gulick, S.P.S., Johnson, K.R., Kiessling, W., Koeberl, C., Kring, D.A., MacLeod, K.G., Matsui, T., Melosh, J., Montanari, A., Morgan, J. V., Neal, C.R., Nichols, D.J., Norris, R.D., Pierazzo, E., Ravizza, G., Rebolledo-Vieyra, M., Reimold, W.U., Robin, E., Salge, T., Speijer, R.P., Sweet, A.R., Urrutia-Fucugauchi, J., Vajda, V., Whalen, M.T., Willumsen, P.S., 2010. The Chicxulub Asteroid Impact and Mass Extinction at the Cretaceous-Paleogene Boundary. Science (1979). 327, 1214–1218. https://doi.org/10.1126/science.1177265

Slama, J., Kosler, J., Condon, D.J., Crowley, J.L., Gerdes, A., Hanchar, J. M. Horstwood, M. S. A. Morris, G.A., Nasdala, L., Norberg, N., Schaltegger, U. Schoene, N., Tubrett, M. N. Whitehouse, M.J., 2008. Plesovice zircon - a new natural reference material for U-Pb and Hf isotopic microanalysis. Chem. Geol. 249, 1–35.

Stacey, J.S., Kramers, J.D., 1975. Approximation of terrestrial lead isotope evolution by a two-stage model. Earth Planet. Sci. Lett. 26, 207–221. https://doi.org/10.1016/0012-821X(75)90088-6

Subarkah, D., Blades, M.L., Collins, A.S., Farkaš, J., Gilbert, S., Löhr, S.C., Redaa, A., Cassidy, E., Zack, T., 2022. Unraveling the histories of Proterozoic shales through *in situ* Rb-Sr dating and trace element laser ablation analysis. Geology 50, 66–70. https://doi.org/10.1130/G49187.1

Thomson, S.N., Gehrels, G.E., Ruiz, J., Buchwaldt, R., 2012. Routine low-damage apatite U-Pb dating using laser ablation–multicollector–ICPMS. Geochemistry, Geophysics, Geosystems 13.

Tillberg, M., Drake, H., Zack, T., Kooijman, E., Whitehouse, M.J., Åström, M.E., 2020. In situ Rb-Sr dating of slickenfibres in deep crystalline basement faults. Sci. Rep. 10, 562. https://doi.org/10.1038/s41598-019-57262-5

Timms, N.E., Erickson, T.M., Pearce, M.A., Cavosie, A.J., Schmieder, M., Tohver, E., Reddy, S.M., Zanetti, M.R., Nemchin, A.A., Wittmann, A., 2017. A pressure-temperature phase diagram for zircon at extreme conditions. Earth. Sci. Rev. 165, 185–202. https://doi.org/10.1016/j.earscirev.2016.12.008

Tollefson, K., Larson, K., 2026. Investigation of the effects of ductile deformation on *in situ* biotite and muscovite Rb-Sr geochronology. Geol. Mag. 163, e22. https://doi.org/10.1017/S0016756826100685

Tollefson, K.T., Larson, K.P., Moynihan, D.P., Cleven, N.R., 2025. In situ mica Rb–Sr geochronology and microstructural analysis to evaluate the timing and sense of shear zone movement: Shannon and d'Abbadie Faults, Yukon, Canada. Can. J. Earth Sci. 62, 1320–1341. https://doi.org/10.1139/cjes-2024-0144

Tuchscherer, M.G., Spray, J.G., 2002. Geology, Mineralization, and Emplacement of the Foy Offset Dike, Sudbury Impact Structure*. Economic Geology 97, 1377–1397. https://doi.org/10.2113/gsecongeo.97.7.1377

Vermeesch, P., 2018. IsoplotR: A free and open toolbox for geochronology. Geoscience Frontiers2 9, 1479–1493.

Villa, I.M., De Bièvre, P., Holden, N.E., Renne, P.R., 2015. IUPAC-IUGS recommendation on the half life of 87Rb. Geochim. Cosmochim. Acta 164, 382–385. https://doi.org/10.1016/j.gca.2015.05.025

https://doi.org/10.5194/egusphere-2026-3441
Preprint. Discussion started: 25 June 2026
© Author(s) 2026. CC BY 4.0 License.

Webb, A.W., Coats, R.P., Fanning, C.M., Flint, R.B., 1983. Geochronological framework of the Adelaide Geosyncline, in: Geological Society of Australia Abstracts.

Williams, G.E., 1992. Acraman: A major impact structure from the Neoproterozoic of Australia. pp. 209–224. https://doi.org/10.1130/SPE293-p209

Williams, G.E., 1986. The Acraman Impact Structure: Source of Ejecta in Late Precambrian Shales, South Australia. Science (1979). 233, 200–203. https://doi.org/10.1126/science.233.4760.200

Williams, G.E., Schmidt, P.W., 2021. Dating the Acraman asteroid impact, South Australia: the case for deep drilling the 'hot shock' zone of the central uplift. Australian Journal of Earth Sciences 68, 355–367. https://doi.org/10.1080/08120099.2020.1808066

Williams, GeorgeE., Wallace, MalcolmW., 2003. The Acraman asteroid impact, South Australia: magnitude and implications for the late Vendian environment. J. Geol. Soc. London. 160, 545–554. https://doi.org/10.1144/0016-764902-142

Woodhead, J.D., Hergt, J.M., 2005. A Preliminary Appraisal of Seven Natural Zircon Reference Materials for In Situ Hf Isotope Determination. Geostand. Geoanal. Res. 29, 183–195.

Woodhead, J.D., Hergt, J.M., 2001. Strontium, Neodymium and Lead Isotope Analyses of NIST Glass Certified Reference Materials: SRM 610, 612, 614. Geostand. Geoanal. Res. 25, 261–266. https://doi.org/10.1111/j.1751-908X.2001.tb00601.x

Zack, T., Hogmalm, K.J., 2016. Laser ablation Rb/Sr dating by online chemical separation of Rb and Sr in an oxygen-filled reaction cell. Chem. Geol. 437, 120–133. https://doi.org/10.1016/j.chemgeo.2016.05.027

Zametzer, A., Kirkland, C.L., Barham, M., Hartnady, M.I.H., Bath, A.B., Rankenburg, K., 2022. Episodic alteration within a gold-bearing Archean shear zone revealed by in situ biotite Rb–Sr dating. Precambrian Res. 382, 106872. https://doi.org/10.1016/j.precamres.2022.106872

https://doi.org/10.5194/egusphere-2026-3441
Preprint. Discussion started: 25 June 2026
© Author(s) 2026. CC BY 4.0 License.

843 **FIGURES**

844

845 Figure 1. Geological context of the Gosses Bluff and Acraman impact sites in respect to the
846 Australian main geological provinces, including the extent of the ejecta layer of the Acraman
847 impact (Bunyeroo Formation).

https://doi.org/10.5194/egusphere-2026-3441
Preprint. Discussion started: 25 June 2026
© Author(s) 2026. CC BY 4.0 License.

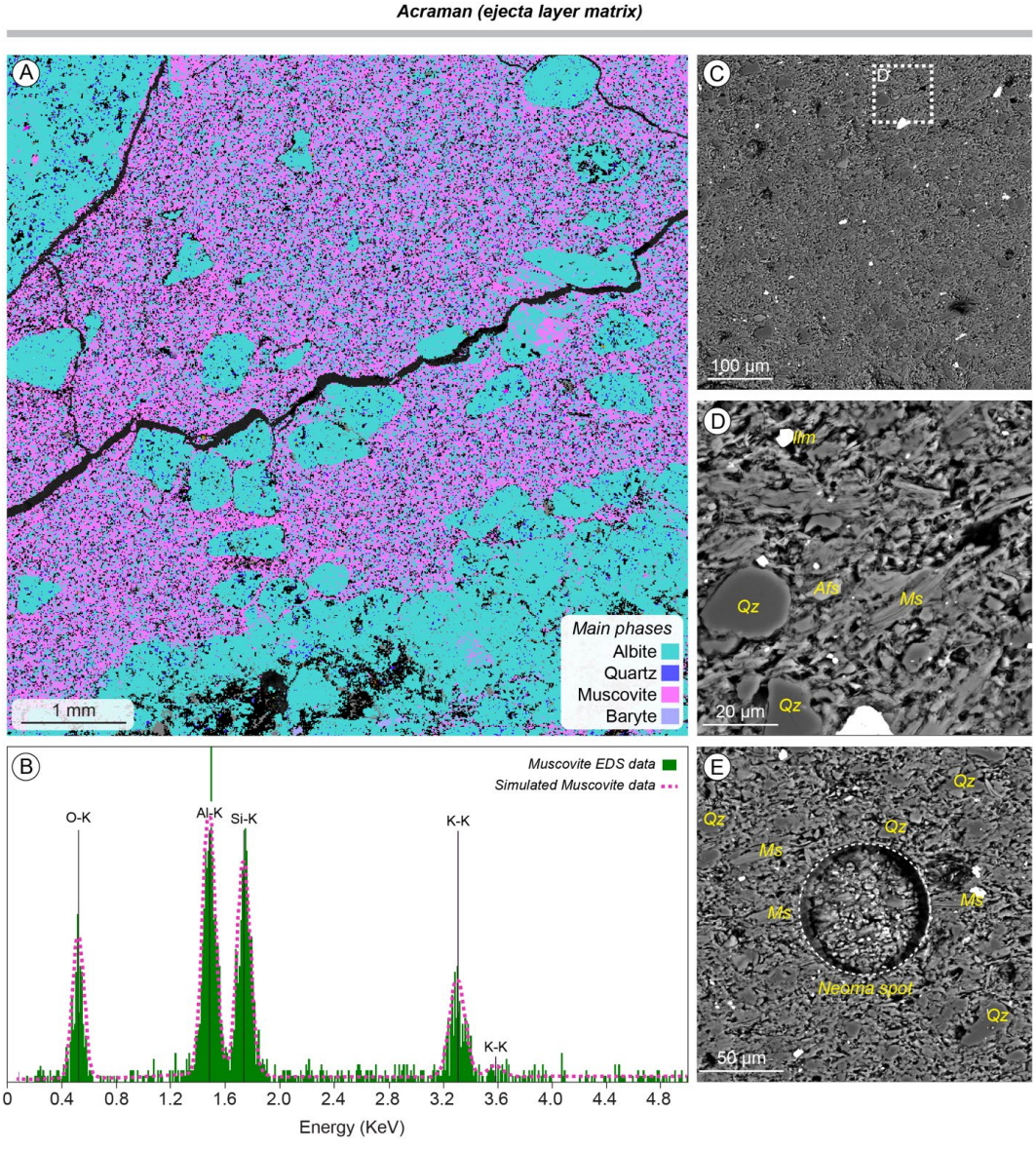

Figure 2. A) TIMA-based mineral phase map of the Acraman sample; B) Muscovite EDS spectra compared to simulated data, highlighting the peaks of major components (K-energy level); C-E) electron backscattered photomicrographs of the fine-grained muscovite domain. The laser-Neoma spot in panels (D) and (E) are 90 µm in diameter. Mineral abbreviations follow Whitney and Evans (2010).

https://doi.org/10.5194/egusphere-2026-3441
Preprint. Discussion started: 25 June 2026
© Author(s) 2026. CC BY 4.0 License.

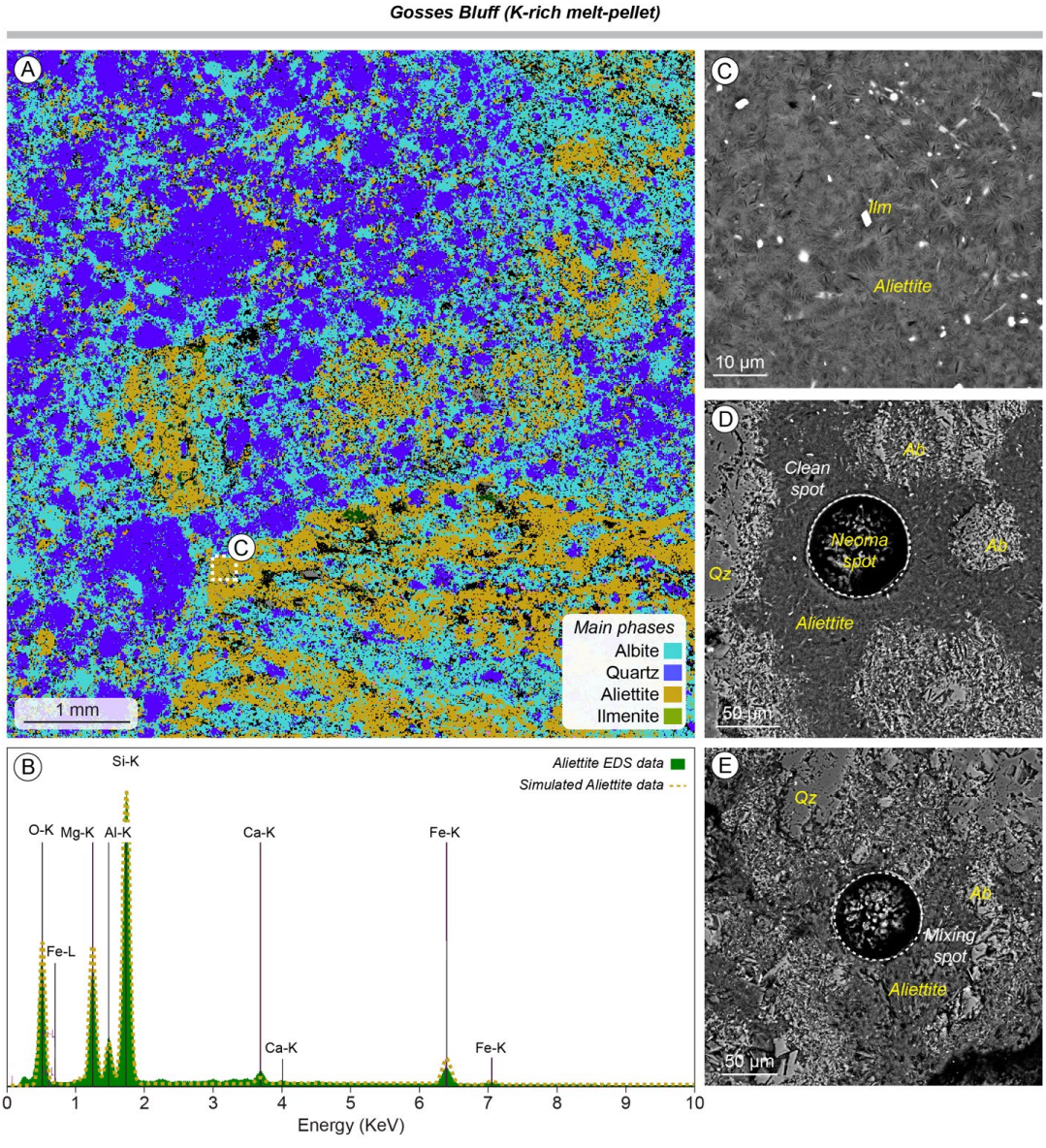

Figure 3. A) TIMA-based mineral phase map of the Gosses Bluff sample; B) Aliettite EDS spectra compared to simulated data, highlighting the peaks of major components (K-energy level); C-E) electron backscattered photomicrographs of the fine-grained aliettite domains. The laser-Neoma spot in panels (D) and (E) are 90 µm in diameter. Mineral abbreviations follow Whitney and Evans (2010).

https://doi.org/10.5194/egusphere-2026-3441
Preprint. Discussion started: 25 June 2026
© Author(s) 2026. CC BY 4.0 License.

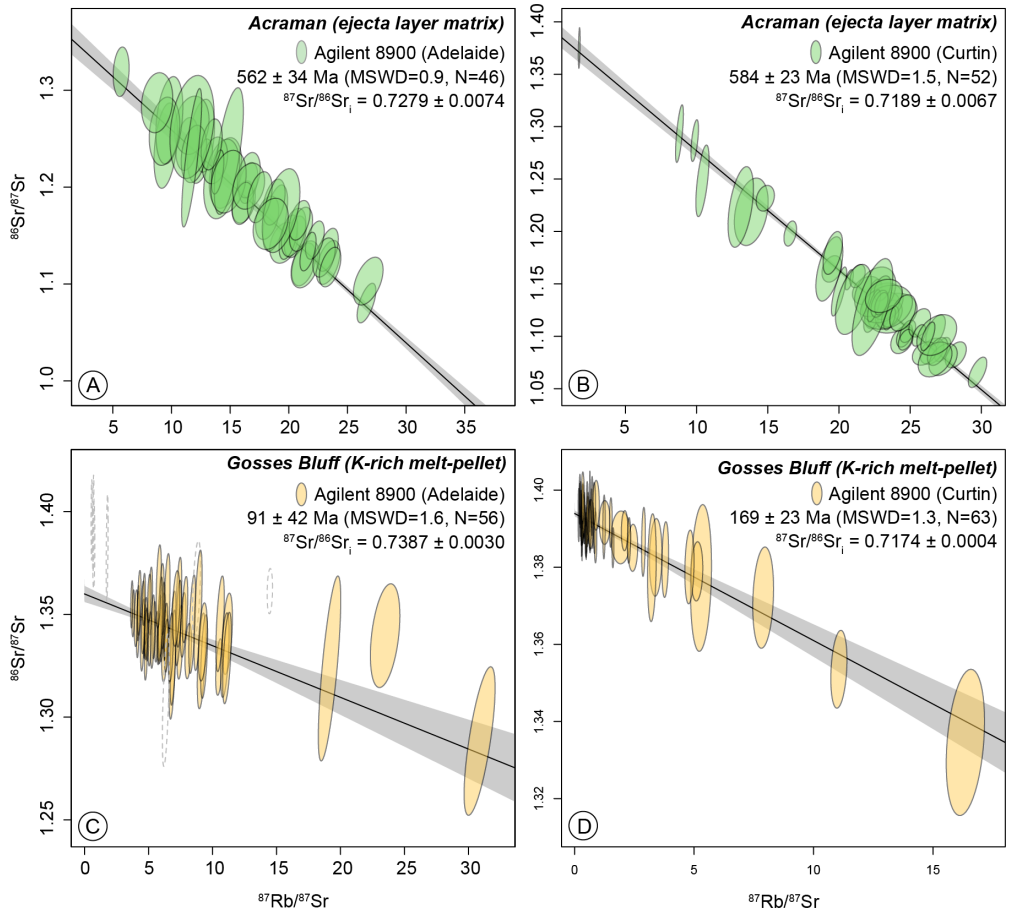

Figure 4. In situ single-collector Rb-Sr data from the Acraman (A, B) and Gosses Bluff (C, D) impact samples. Left panels display the Rb–Sr data obtained at the University of Adelaide, whilst the right panels display the data obtained at Curtin University. Uncertainties are presented at 2-standard error.

https://doi.org/10.5194/egusphere-2026-3441
Preprint. Discussion started: 25 June 2026
© Author(s) 2026. CC BY 4.0 License.

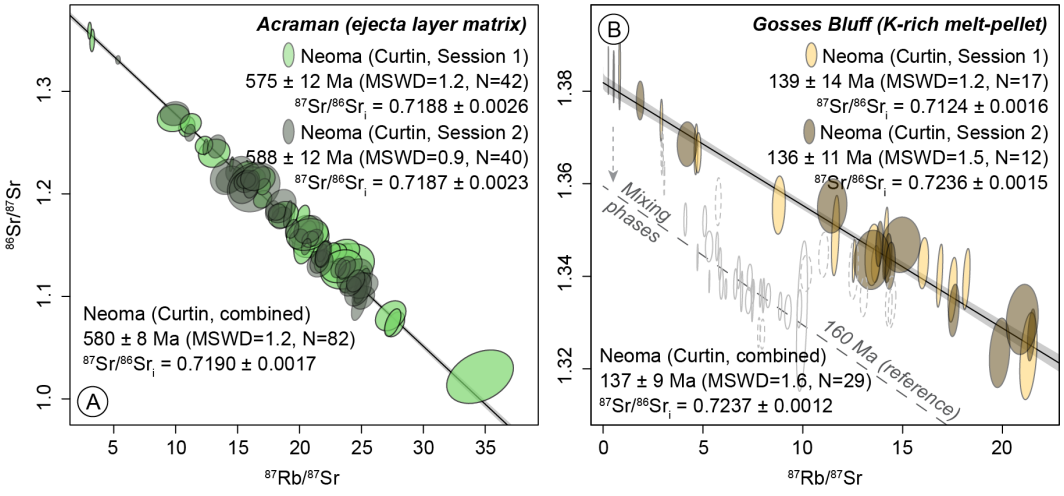

Figure 5. In situ multi-collector Rb-Sr data from the Acraman and Gosses Bluff impact samples. Uncertainties are presented at 2-standard error.

https://doi.org/10.5194/egusphere-2026-3441
Preprint. Discussion started: 25 June 2026
© Author(s) 2026. CC BY 4.0 License.

884

885

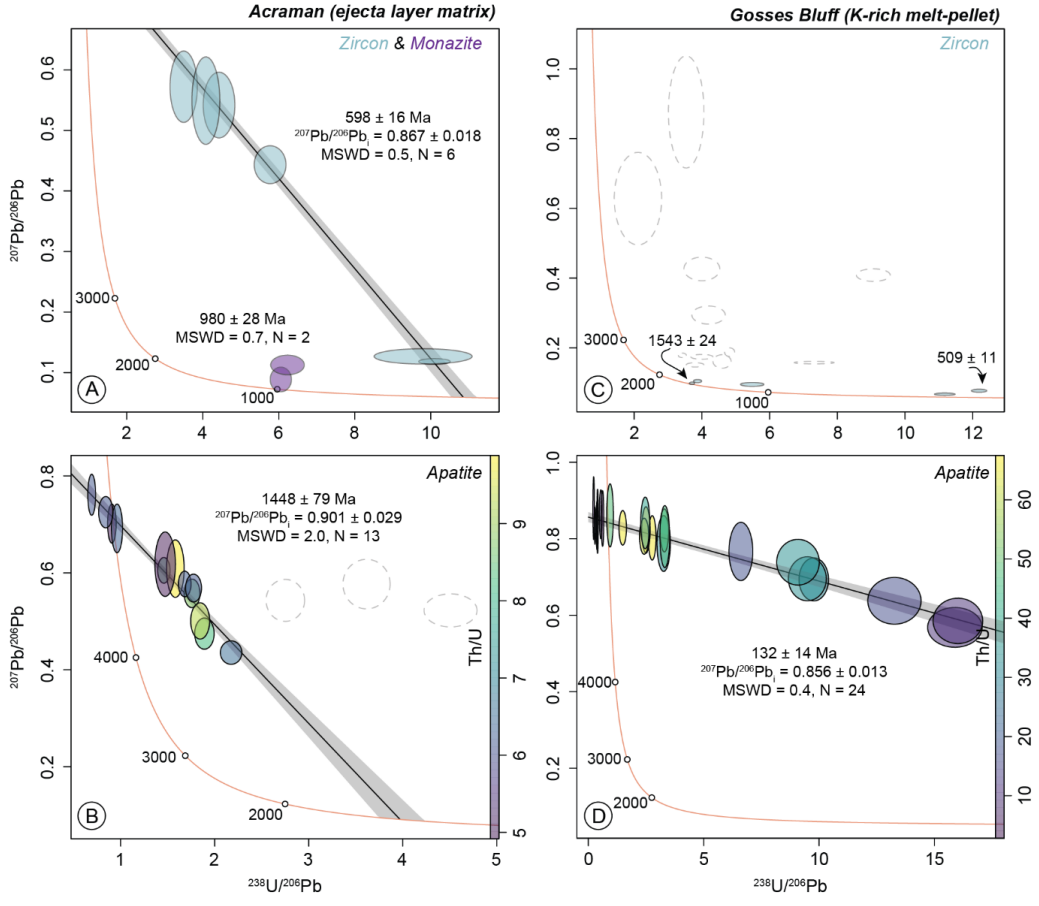

886

887 Figure 6. A) Monazite and zircon, and B) apatite U–Pb data from the Acraman ejecta layer. C)

888 Zircon and (D) apatite U–Pb data from the Gosses Bluff K-rich melt pellet. Uncertainties are

889 presented at 2-standard error.

890

https://doi.org/10.5194/egusphere-2026-3441
Preprint. Discussion started: 25 June 2026
© Author(s) 2026. CC BY 4.0 License.

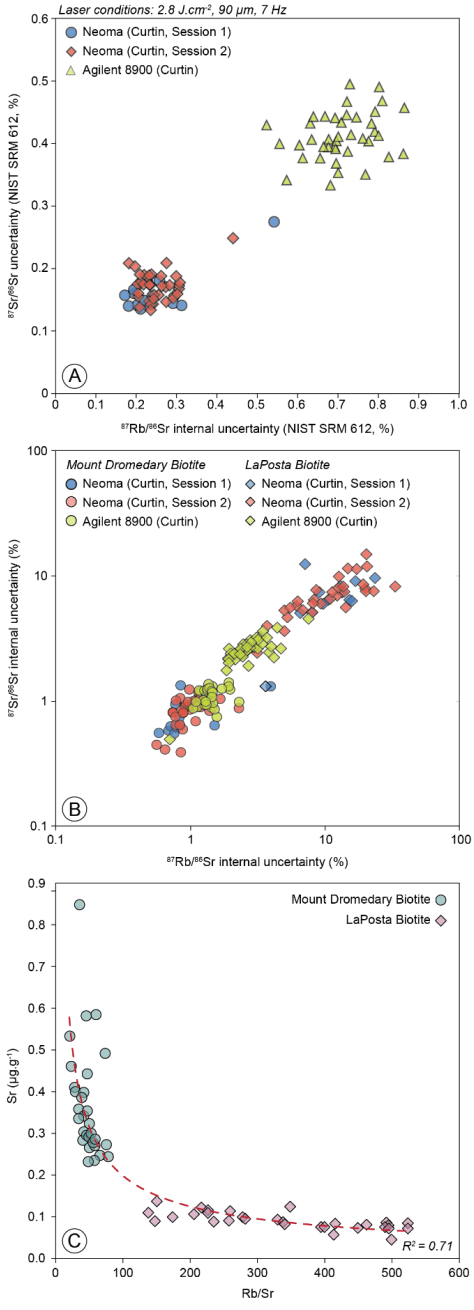

Figure 7. Analytical comparison between single- and multi-collector mass spectrometers, including (A) the measurement of $^{87}Sr/^{86}Sr$ and $^{87}Sr/^{86}Sr$ measurements on NIST SRM 612, and (B) natural mica reference materials (Mount Dromedary and LaPosta biotite).

https://doi.org/10.5194/egusphere-2026-3441
Preprint. Discussion started: 25 June 2026
© Author(s) 2026. CC BY 4.0 License.

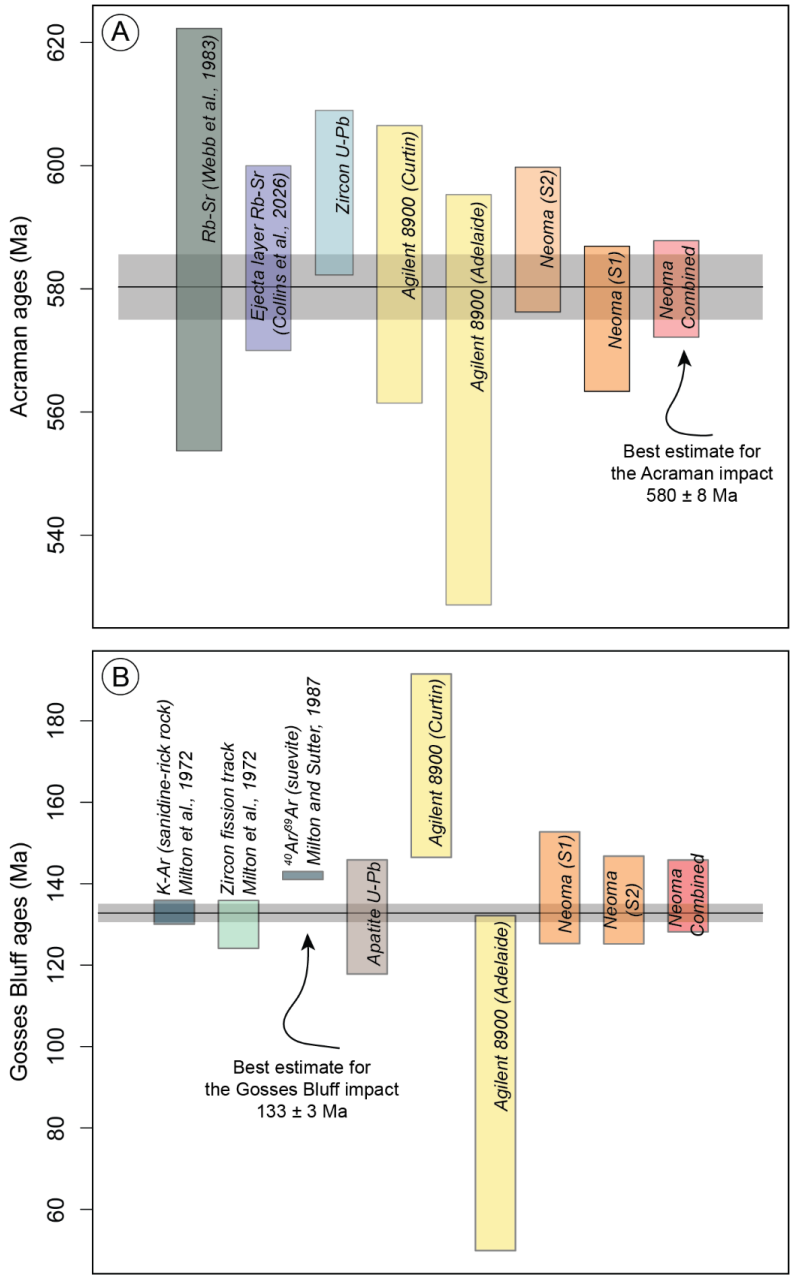

Figure 8. Comparison between new ages from the Acraman (A) and Gosses Bluff (B) impact and available literature data from both sites (Milton et al., 1972; Webb et al., 1983; Milton and Sutter, 1987; Collins et al., 2026).